# SOLVENT-INDUCED CHANGES IN MOLECULAR CONFORMATION AND AGGREGATION STUDIED BY ION MOBILITY EXPERIMENTS

Jeffrey A. Everett

Submitted to the faculty of the University Graduate School in partial fulfillment of the requirements for the degree

Master of Science in the Department of Chemistry,

Indiana University

May 2012

Accepted by the Graduate Faculty, Indiana University, in partial fulfillment of for the degree of Master of Science in Chemistry.	the requirements
Master of Science Committee	
David E. Clemmer, Ph.D., Professor of C	
	memistry (ddvisor)
Lane A. Baker, Ph.D., Profe	essor of Chemistry
Inasmuch as this candidate has completed all other requirements, I recommen	
Department of Chemistry that, upon completion of the course program, he be of Master of Science in Chemistry.  Director of Graduate Studies	granted the degree
Caroline C. Jarrold, Ph.D., Profe	essor of Chemistry

Copyright © 2012 Jeffrey A. Everett

### **Dedication**

To my parents, Timothy and Pamela Everett, who have consistently supported all of my various endeavors, and fostered my academic interests. To my wife, Meghan McCormick, who has encouraged my academic growth, and provided constant emotional support. And, finally, to the men of Tau Kappa Epsilon, who have fostered my personal growth and served to expand my view of the world that surrounds me.



mutatis mutandis

### Acknowledgments

I would like to personally thank and recognize the various people and organizations that have helped to complete this project. First, I would like to thank my advisor, Dr. David E. Clemmer, for this opportunity and all of the guidance and support he has provided. I would also like to thank the remaining members of my graduate committee, Dr. James P. Reilly, Dr. Lane A. Baker, and Dr. Liang-shi Li for all of the guidance they have provided. Additionally, I would like to thank all of the Clemmer group members, especially Dr. Stephen J. Valentine, for their consistent support and constant source of ideas and discussion. Of these many colleagues, I would like to thank Nicholas A. Pierson for his help in starting the original angiotensin I project and Natalya Atlasevich for her expertise in understanding aggregation phenomena. Furthermore, I would like to thank Steven M. Zucker, Michael A. Ewing, Jonathan M. Dilger and Rebecca S. Glaskin for their reliable source of ideas, discussion, and overall support throughout my graduate career. Much of this work would not be possible without the fine work of Mr. Gary Fleener and the rest of the Mechanical Instrument Services team, Mr. John Poehlman and his team in Electronic Instrument Services, or Mr. Brian Crouch and his team in the Information Technology Group. Lastly, I would like to thank all of my supportive friends and family who have helped me get to where I am today.

## Solvent-Induced Changes in Molecular Conformation and Aggregation Studied by Ion Mobility Experiments

Jeffrey A. Everett

The aggregation of peptides and proteins has been shown to be involved in the development of numerous degenerative conditions including Parkinson's and Alzheimer's diseases. However, little is known about how or why these specific aggregates are formed. One significant problem that exists in attempting to measure the structure and formation of these aggregates involves the rapid interconversion of structural conformations in solution. In order to overcome this difficulty, experiments have been performed in the gas phase because of the concomitant reduction in intermolecular interactions and the stabilization of the structure brought on by the 'freezing-out' of structures as they enter the gas phase.

Multidimensional ion mobility spectrometry has been coupled with mass spectrometry in order to measure the influence of solution conditions on the gas phase structures of the  $[M+3H]^{3+}$  ion of angiotensin I. In many solution conditions, only a single stable gas-phase structure is observed, however, solutions containing dimethyl sulfoxide produce three distinct gas-phase conformers. Individually selecting and collisionally activating each of the three conformations, results in the conversion of the two elongated structures into the previously observed stable gas-phase conformation. This suggests that although the  $[M+3H]^{3+}$  ion has a single stable gas-phase structure, certain structural elements derived from solution-phase antecedents may be retained and observed in the gas phase. We have further employed these ion mobility measurements as a high-throughput method for monitoring the aggregation process of angiotensin II showing the accumulation of monomers into dimers and trimers. Here, gas-phase measurements allow nearly real-time monitoring of the electrospray formation of  $[nM+nH]^{n+}$  ions of angiotensin II from solutions containing polyfluorinated alcohols.

## **Table of Contents**

Dedication	1V
Acknowledgments	v
Abstract	vi
Table of Contents	vii
List of Figures	ix
List of Tables	xi
Chapter 1 – Introduction	1
Background	1
Ion mobility as a high-throughput method of structural characterization	1
Influence of solvent on ion conformations	3
References	7
Chapter 2 – Influence of Solution Composition on Gas-Phase Structure of Angiotensin I  Determined by Ion Mobility Measurements	11
Introduction	11
Experimental Methods	14
General	14
Selection and Activation.	15
Calculating Collisional Cross-Sections.	17
Results and Discussion	17
Solutions Containing Trifluoroethanol and Dimethyl Sulfoxide	17
Conformational Changes Observed Upon Activation in DMSO	23
Implications of DMSO and TFE as Solvents	28
Conclusions	29
Acknowledgements	29
References	30
Chapter 3 – Aggregation of Angiotensin II Monitored in Real Time by Ion Mobility  Spectrometry	36
Introduction	36
Experimental	38
General	38

	ESI Solution Conditions	40
	Data Analysis	40
	Results and Discussion	41
	Preliminary Aggregation Observations	41
	Dissociation of Aggregates	46
	Time-Dependent Formation of Aggregates	48
	Considerations for Further Investigation	51
	Conclusions	52
	Acknowledgements	53
	References	54
Appendix A.		57
	References	61
Appendix B.		62
	Introduction	62
	Experimental	62
	General	62
	NAMD Parameters	63
	Collisional Cross-Section Calculation	63
	Preliminary Results and Discussion	63
	Conclusions	64
	Acknowledgements	65
	References	67

## **List of Figures**

<b>Figure 2.1</b> : Schematic diagram of the IMS–IMS–MS instrument consisting of a robotic autosampler ESI source, a ~1.8 m drift tube (D1 and D2), and a time-of-flight mass spectrometer
<b>Figure 2.2</b> : Two dimensional plot representing nested $m/z$ measurements within drift time measurements for angiotensin I in a 50:50 methanol:water solution. Compressions of each dimension are shown on the $x$ - and $y$ -axes, representing total ion drift time distribution and mass spectrum, respectively. The pressure of the He buffer gas was maintained at $\sim 3.10$ Torr at 300 K
<b>Figure 2.3</b> : <b>(A)</b> Stacked drift profiles for the [M+3H] <sup>3+</sup> ions of angiotensin I plotted on a raw drift time scale as a function of increasing concentration of TFE from pure water solutions up to 90% (by volume) TFE. <b>(B)</b> Stacked drift profiles for the [M+3H] <sup>3+</sup> ions of angiotensin I plotted on a drift time scale as a function of increasing concentration of DMSO from pure water solutions up to 70% (by volume) DMSO. For all experiments represented in the figure the He buffer gas was maintained at a pressure of ~3.5 Torr
<b>Figure 2.4</b> : Stacked drift profiles for the $[M+3H]^{3+}$ ion of angiotensin I plotted on a drift time scale as a function of solvent composition. Here, the influence of each solvent is compared directly for 50:50 (% volume) mixtures of solvent and water. For all experiments represented in the figure the He buffer gas was maintained at a pressure of $\sim 3.5$ Torr
<b>Figure 2.5</b> : Drift profiles of the [M+3H] <sup>3+</sup> angiotensin I ion plotted on a drift time scale. The bottom curve in each panel shows the ESI source distribution obtained for the 25:75 (% volume) DMSO:water. The individual panels (arbitrarily assigned A through C) show one of three separate experiments beginning with the initial selection of a conformation with no activation followed by successively increasing activation voltages up to 150 V. Activation voltages greater than 150 V result in subsequent fragmentation of the target ion and are therefore omitted. For all experiments the He buffer gas was maintained at a pressure of ~3.0 Torr. Selections of the three conformers A through C all converge to the same distribution of the stable conformer A at an activation voltage of 50 V.
<b>Figure 3.1</b> : Schematic diagram of the IMS–IMS–MS instrument consisting of a robotic autosampler ESI source, a ~1.8 m drift tube (D1 and D2), and a time-of-flight mass spectrometer.

**Figure 3.2**: Characteristic two-dimensional (2D) representation of mass-to-charge (m/z) ratio measurements nested within drift time measurements for the 60 minute incubation experiment.

The	three	charge	states	of	interest	are	labeled	accordingly	and	relative	signal	intensit	y is
repre	esentec	d by col	or, who	ere	cooler co	olors	such as	navy blue r	epres	ent low	ion cou	nts and	reds
indi	cate hig	gh ion c	ounts.	Γhe	drift pre	ssure	e was hel	ld constant at	~3.1	0 Torr H	[e		42

**Figure 3.3**: Extracted drift profiles for the  $[nM+nH]^{n+}$  species of angiotensin II plotted on a drift time scale. Experiments were performed with individual  $\sim$ 0.95 mM solutions containing equal parts (by volume) ACN and water or TFE and water. Multimer identification is possible by extracting the mass spectral data from each of the distributions and analyzing the isotopic distribution. For both experiments the He buffer gas was maintained at a pressure of  $\sim$ 3.5 Torr. As shown here, it is possible to identify individual species up to trimers in solutions of TFE and tetramers in solutions of ACN, although evidence for higher-order aggregates is also observed.44

**Figure 3.6**: Calculated and normalized peak area represented as a function of incubation time for each of the four species of angiotensin II of interest. Significantly more measurements are included for the first 660 minutes than for the ~8400 minutes that follow. In order to observe the long time steps on the same plot as the many shorter time measurements within the first 11 hours, incubation time is represented on a logarithm scale. The overlaid lines are not intended to be accurate curve fits, but are only included in order to draw attention to the approximate trends within the data points for illustrative purposes.

**Figure B.1**: Calculated collisional cross-section (CCS) plotted on a time scale. The red line represents the raw calculations for all 4000 conformations as a function of simulation time. The black line is a moving average (n = 10) illustrating the general trend of the calculations. Dashed lines representing the three experimentally determined collisional cross-sections for each of the conformers (A–C) of angiotensin I in DMSO:water are overlaid. The inset figure shows the same MD calculation performed on a shortened time scale without the presence of DMSO, where an overall decrease in CCS is observed.

## **List of Tables**

<b>Table</b>	<b>A.1</b> :	Tabulated	l physical	properties	of the	six	analytical	solvents	investigated	during	the
course	of th	e experim	ents descr	ibed in Cha	apter 2	and	Chapter 3.				58

# Chapter 1 – Introduction Background

The study of protein and peptide aggregation in biological systems has gained increased consideration as a result of the role of oligomers and fibrils in the development of neurodegenerative disorders including Parkinson's and Alzheimer's diseases. Although it is known that even small protein oligomers can cause irreversible neuronal injuries, the mechanism associated with the self-assembly of these proteins is still a matter of debate. Recently, it has been shown that many generic proteins or peptides can form ordered aggregates under suitable conditions, though these conditions may vary slightly for individual molecules. The relationship among the structures of the polypeptides, the surrounding environment, and the formation of aggregation products is relatively difficult to study in the solution phase due to the rapid interconversion of structural conformers. Some experiments suggest that the transition from the solution phase into the gas phase during the electrospray ionization (ESI)<sup>5</sup> process involves the rapid removal of solvent molecules, resulting in stabilization of specific structures — commonly referred to as *freezing out* due to the cooling effects of evaporation — and an overall reduction in structural interconversion.

### Ion mobility as a high-throughput method of structural characterization

Since the initial development of ESI as a "soft" ionization technique for mass spectrometry (MS), a number of studies and experiments have been performed in an attempt to understand the structures of the solvent-free ions that are produced.<sup>7-17</sup> As an extension of these studies, it is important to be able to link the gas-phase structures of these ions with those of their solution-phase antecedents. One technique that has emerged for the characterization of gas-phase ion conformations is ion mobility spectrometry (IMS).<sup>16</sup> Although IMS is a relatively established

technique, it has experienced a substantial renaissance over the past two decades.<sup>18</sup> When coupled with mass spectrometry, traditional IMS offers the distinctive capability to differentiate multiple conformations of ions of a single mass-to-charge (*m/z*) species. This resolution capability allows for the identification of aggregates and multimers that are difficult or impossible to observe by MS alone.<sup>19</sup> The recent development of higher order IMS techniques including two-dimensional IMS (IMS–IMS), and three-dimensional (IMS–IMS–IMS) has allowed probing of the activation energies required to induce structural transitions between various conformations and ultimately differentiate between energetically-stable gas-phase conformers and those derived from other solution-phase structures.<sup>20</sup>

The development of faster and more powerful computing systems and modeling software has helped to increase the relevance of ion mobility measurements by allowing rapid and increasingly detailed structural simulations such that the experimentally determined collision cross-sections can be compared with those calculated from structures that are obtained from molecular dynamics (MD) simulations. While traditional solution-phase measurements such as gel electrophoresis can be used to determine which oligomeric aggregates are formed, it becomes difficult, if not impossible, to accurately obtain structural or orientational information. In the studies presented here, IMS measurements coupled with MS can be used to quickly and directly study aggregation phenomena in real time. In ideal cases, it becomes possible to swiftly identify and characterize varying degrees of oligomerization from dimers to pentamers, and in rare cases even larger aggregates can be identified and studied.

#### Influence of solvent on ion conformations

McLafferty and co-workers first illustrated the connection between gas-phase and solution-phase biomolecular conformations through hydrogen-deuterium ( $^{1}$ H/ $^{2}$ H) exchange experiments performed within a high-resolution Fourier-transform ion-cyclotron-resonance (FT–ICR) mass spectrometer. In these experiments, they were able to observe gas-phase conformations of cytochrome c directly corresponding to known conformations previously observed in solution. Further investigations by Jarrold and Clemmer have shown that it is possible to observe multiple partially-folded transition-state conformations of cytochrome c in the gas phase that are not easily observed with nuclear magnetic resonance (NMR) or x-ray crystallography methods. c

Additionally, Loo and co-workers have previously shown a correlation between the higher-order structures of gas- and solution-phase biomolecular ions<sup>21</sup> and other recent reports from Robinson, Bowers, and their collaborators suggest that the gas-phase conformations of large non-covalent complexes may reflect their original solution-phase structures.<sup>22-24</sup> Previous studies have also shown that the number and relative abundance of different solution conformations observed in ion mobility experiments are related to the electrospray solution composition.<sup>25, 26</sup>

The experiments described here focus on two distinctive ions of the angiotensin I and angiotensin II series. Angiotensin I (AGT I; Asp–Arg–Val–Tyr–Ile–His–Pro–Phe–His–Leu–OH) is an important intermediate peptide in the renin–angiotensin system<sup>27</sup> formed in the blood stream through the enzymatic cleavage of the large precursor glycoprotein angiotensinogen by renin. Although angiotensin I is biologically-inactive, it is quickly cleaved into the biologically-

active octapeptide angiotensin II (AGT II; Asp–Arg–Val–Tyr–Ile–His–Pro–Phe–OH) by converting enzymes located on the luminal surfaces of endothelial cells.<sup>28</sup>

The renin–angiotensin system is responsible for a variety of biological processes within the body, but its ability to increase blood pressure, which has been shown to lead to hypertension, heart failure and various renal diseases, has attracted considerable pharmaceutical interest.<sup>29, 30</sup> As a result, a significant amount of work has been done to elucidate the solution structure of angiotensin II, and its analogues, involving a variety of techniques including circular dichroism (CD),<sup>31-34</sup> nuclear magnetic resonance ( $^{1}$ H and  $^{13}$ C NMR),<sup>31-40</sup> infrared (IR) and Raman spectroscopy,<sup>41, 42</sup> hydrogen–deuterium exchange (HDX)<sup>43</sup> and various conformational calculations.<sup>44-47</sup> These studies have proposed a wide variety of structures including  $\alpha$ -helices,<sup>48, 49</sup>  $\beta$ -pleated sheets, and both  $\beta$ - and  $\gamma$ -turns<sup>42, 50</sup> such that the number of proposed structures is significantly disproportionate to the length of the peptide itself.<sup>40</sup>

Considerably less work has been done to elucidate the structure of the precursor angiotensin I. Although extensive studies have led to many conformational models for the smaller angiotensin II, few structures have been described for the precursor angiotensin I, and only recently was an experimentally determined structure reported. However, as both peptides share a common N-terminal and differ only in length and the C-terminal configuration due to the presence or absence of the His<sup>9</sup>–Leu<sup>10</sup> dipeptide, it is possible that a portion of the structure is preserved between the two peptides. Described to the elucidate the structure of the precursor angiotensin I.

Chapter 2 focuses on the experimental work performed on the [M+3H]<sup>3+</sup> ion of angiotensin I produced by electrospray ionization from a variety of common organic solvents. Previous work has characterized the [M+3H]<sup>3+</sup> bradykinin ion originating from different solvent conditions consisting of water/methanol and water/dioxane mixtures. 25, 26 As an extension of this early work, two additional organic solvents — dimethyl sulfoxide (DMSO) and 2,2,2-trifluoroethanol (TFE) — were selected as a result of their prevalence as NMR solvents and their tendency to favor compact conformations of angiotensin II analogs and derivatives. 40, 42 DMSO has also been used in previous NMR experiments with various angiotensin analogues to simulate aprotic receptor environments<sup>46, 51</sup> and eliminate multiple conformational isomers.<sup>52</sup> Similarly, TFE has been extensively used as a co-solvent for the study of peptides due to its ability to stabilize or induce the formation of elements of secondary structure, leading to the observation of  $\alpha$ -helices and β-sheets in NMR and CD studies. 53-55 Both TFE and DMSO have been identified as relatively useful membrane-mimetic organic solvents due to their relatively small dielectric constants, and large dipole moments (Table A.1).<sup>56</sup> However, DMSO is also known to cause unfolding or denaturation of peptides above a certain concentration due to the disruption of the intramolecular hydrogen bonds along the backbone.<sup>57</sup> The results described here suggest that this characteristic unfolding may result in the formation of additional structures that can be observed in the gas-phase. Upon mobility selection and activation these additional structures are observed to collapse to a single stable gas-phase structure. The data suggest that one of the derived gasphase structures arising from multiple solution conformations is significantly more stable than the others.

Chapter 3 describes a second set of experiments that demonstrate angiotensin II readily forming identifiable oligomerized species of  $[nM+nH]^{n+}$  ions from a variety of organic solvents. Further investigation of these aggregation species suggests that their presence is due in part to the manufacturing and purification processes, and exist prior to the initial analysis. Upon dissociation of these pre-formed aggregation products with polyfluorinated alcohols, it is possible to observe the formation of different aggregate species over time, with higher-order aggregates increasing over time. In these experiments, the high-throughput nature of ion mobility measurements allows these aggregation phenomena to be observed in near real-time while maintaining a certain degree of the native solution structure of the peptide that is often lost when using other techniques.

#### References

- 1. Kirkitadze, M. D.; Bitan, G.; Teplow, D. B., *J. Neurosci. Res.* **2002**, *69*, 567–577.
- 2. Lashuel, H. A.; Hartley, D.; Petre, B. M.; Walz, T.; Lansbury, P. T., *Nature* **2002**, *418*, 291–291.
- 3. Kłoniecki, M.; Jabłonowska, A.; Poznański, J.; Langridge, J.; Hughes, C.; Campuzano, I.; Giles, K.; Dadlez, M., *J. Mol. Biol.* **2011**, *407*, 110–124.
- 4. Thirumalai, D.; Klimov, D.; Dima, R., Curr. Opin. Struct. Biol. 2003, 13, 146–159.
- 5. Fenn, J. B.; Mann, M.; Meng, C. K.; Wong, S. F.; Whitehouse, C. M., *Science* **1989**, *246*, 64–71.
- 6. Lee, S.-W.; Freivogel, P.; Schindler, T.; Beauchamp, J. L., *J. Am. Chem. Soc.* **1998**, *120*, 11758–11765.
- 7. Chowdhury, S. K.; Chait, B. T., *Biochem. Biophys. Res. Commun.* **1990**, *173*, 927–931.
- 8. Katta, V.; Chait, B. T., *Rapid Commun. Mass Spectrom.* **1991**, *5*, 214–217.
- 9. Suckau, D.; Shi, Y.; Beu, S. C.; Senko, M. W.; Quinn, J. P.; Wampler, F. M.; McLafferty, F. W., *Proc. Natl. Acad. Sci. U. S. A.* **1993**, *90*, 790–793.
- 10. Covey, T.; Douglas, D. J., J. Am. Soc. Mass Spectrom. 1993, 4, 616–623.
- 11. Clemmer, D. E.; Hudgins, R. R.; Jarrold, M. F., J. Am. Chem. Soc. 1995, 117, 10141–10142.
- 12. Vonhelden, G.; Wyttenbach, T.; Bowers, M. T., Science 1995, 267, 1483–1485.
- 13. Bowers, M. T.; Marshall, A. G.; McLafferty, F. W., *J. Phys. Chem.* **1996**, *100*, 12897–12910.
- 14. Smith, R. D.; Bruce, J. E.; Wu, Q. Y.; Lei, Q. P., Chem. Soc. Rev. 1997, 26, 191–202.

- 15. Williams, E. R., *J. Mass Spectrom.* **1996**, *31*, 831–842.
- 16. Hoaglund-Hyzer, C. S.; Counterman, A. E.; Clemmer, D. E., *Chem. Rev.* **1999**, *99*, 3037–3079.
- 17. Wyttenbach, T.; Bowers, M. T., Annu. Rev. Phys. Chem. 2007, 58, 511–533.
- 18. Kemper, P. R.; Dupuis, N. F.; Bowers, M. T., *Int. J. Mass. Spectrom.* **2009**, *287*, 46–57.
- 19. Counterman, A. E.; Valentine, S. J.; Srebalus, C. A.; Henderson, S. C.; Hoaglund, C. S.; Clemmer, D. E., *J. Am. Soc. Mass Spectrom.* **1998**, *9*, 743–759.
- Merenbloom, S. I.; Koeniger, S. L.; Valentine, S. J.; Plasencia, M. D.; Clemmer, D. E.,
   Anal. Chem. 2006, 78, 2802–2809.
- 21. Loo, J. A.; He, J. X.; Cody, W. L., J. Am. Chem. Soc. 1998, 120, 4542–4543.
- 22. Ruotolo, B. T.; Verbeck; Thomson, L. M.; Woods, A. S.; Gillig, K. J.; Russell, D. H., *J. Proteome Res.* **2002**, *1*, 303–306.
- 23. Painter, A. J.; Jaya, N.; Basha, E.; Vierling, E.; Robinson, C. V.; Benesch, J. L. P., *Chem. Biol.* **2008**, *15*, 246–253.
- Bernstein, S. L.; Dupuis, N. F.; Lazo, N. D.; Wyttenbach, T.; Condron, M. M.; Bitan, G.;
   Teplow, D. B.; Shea, J.-E.; Ruotolo, B. T.; Robinson, C. V.; Bowers, M. T., *Nat. Chem.* 2009, *1*, 326–331.
- 25. Pierson, N. A.; Valentine, S. J.; Clemmer, D. E., J. Phys. Chem. B **2010**, 114, 7777–7783.
- 26. Pierson, N. A.; Chen, L.; Valentine, S. J.; Russell, D. H.; Clemmer, D. E., *J. Am. Chem. Soc.* **2011**, *133*, 13810–13813.
- 27. Page, I. H.; Bumpus, F. M., *Physiol. Rev.* **1961**, *41*, 331–390.
- 28. Reid, I. A., Arch. Intern. Med. 1985, 145, 1475–1479.
- 29. Regoli, D.; Park, W. K.; Rioux, F., *Pharmacol. Rev.* **1974**, *26*, 69–123.

- 30. Moore, G. J.; Matsoukas, J. M., *Biosci. Rep.* **1985**, *5*, 407–416.
- 31. Fermandjian, S.; Sakarellos, C.; Piriou, F.; Juy, M.; Toma, F.; Thanh, H. L.; Lintner, K.; Khosla, M. C.; Smeby, R. R.; Bumpus, F. M., *Biopolymers* **1983**, *22*, 227–231.
- 32. Fermandjian, S.; Piriou, F.; Sakarellos, C.; Lintner, K.; Khosla, M. C.; Smeby, R. R.; Bumpus, F. M., *Biopolymers* **1981**, *20*, 1971–1983.
- 33. Aumelas, A.; Sakarellos, C.; Lintner, K.; Fermandjian, S.; Khosla, M. C.; Smeby, R. R.; Bumpus, F. M., *Proc. Natl. Acad. Sci. U. S. A.* **1985**, *82*, 1881–1885.
- 34. Khosla, M. C.; Stachowiak, K.; Smeby, R. R.; Bumpus, F. M.; Piriou, F.; Lintner, K.; Fermandjian, S., *Proc. Natl. Acad. Sci. U. S. A.* **1981**, *78*, 757–760.
- 35. Matsoukas, J. M.; Moore, G. J., Arch. Biochem. Biophys. 1986, 248, 419–423.
- 36. Galardy, R. E.; Liakopoulou-Kyriakides, M., Int. J. Pept. Protein Res. 1982, 20, 144–148.
- 37. Lenkinski, R. E.; Stephens, R. L., *J. Inorg. Biochem.* **1983**, *18*, 175–180.
- 38. Matsoukas, J. M.; Bigam, G.; Zhou, N.; Moore, G. J., *Peptides* **1990**, *11*, 359–366.
- 39. Deslauriers, R.; Paiva, A. C. M.; Schaumburg, K.; Smith, I. C. P., *Biochemistry* **1975**, *14*, 878–886.
- 40. Spyroulias, G. A.; Nikolakopoulou, P.; Tzakos, A.; Gerothanassis, I. P.; Magafa, V.; Manessi Zoupa, E.; Cordopatis, P., *Eur. J. Biochem.* **2003**, *270*, 2163–2173.
- 41. Sakarellos, C.; Lintner, K.; Piriou, F.; Fermandjian, S., *Biopolymers* **1983**, *22*, 663–687.
- 42. Fermandjian, S.; Fromageot, P.; Tistchenko, A.-M.; Leicknam, J.-P.; Lutz, M., *Eur. J. Biochem.* **1972**, *28*, 174–182.
- 43. Lenkinski, R. E.; Stephens, R. L.; Krishna, N. R., *Biochemistry* **1981**, *20*, 3122–3126.
- 44. De Coen, J.-L.; Ralston, E., *Biopolymers* **1977**, *16*, 1929–1943.

- 45. Rauk, A.; Hamilton, G.; Moore, G. J., *Biochem. Biophys. Res. Commun.* **1987**, *145*, 1349–1355.
- 46. Joseph, M. P.; Maigret, B.; Scheraga, H. A., Int. J. Pept. Protein Res. 1995, 46, 514–526.
- 47. Preto, M. A. C.; Melo, A.; Maia, H. L. S.; Mavromoustakos, T.; Ramos, M. J., *J. Phys. Chem. B* **2005**, *109*, 17743–17751.
- 48. Krimm, S.; Bandekar, J., Adv. Protein Chem. 1986, 38, 181–364.
- 49. Byler, D. M.; Susi, H., *Biopolymers* **1986**, *25*, 469–487.
- 50. Printz, M. P.; Bleich, H.; Nemethy, G., *Nature-New Biology* **1972**, *237*, 135–140.
- 51. Matsoukas, J. M.; Hondrelis, J.; Keramida, M.; Mavromoustakos, T.; Makriyannis, A.; Yamdagni, R.; Wu, Q.; Moore, G. J., *J. Biol. Chem.* **1994**, *269*, 5303–5312.
- 52. Buck, M., Q. Rev. Biophys. 1998, 31, 297–355.
- 53. Hong, D.-P.; Hoshino, M.; Kuboi, R.; Goto, Y., J. Am. Chem. Soc. 1999, 121, 8427–8433.
- 54. Jasanoff, A.; Fersht, A. R., *Biochemistry* **1994**, *33*, 2129–2135.
- 55. Roccatano, D.; Colombo, G.; Fioroni, M.; Mark, A. E., *Proc. Natl. Acad. Sci. U. S. A.* **2002**, *99*, 12179–12184.
- 56. Chatterjee, A.; Bothra, A. K., *Int. J. Integ. Biol.* **2010**, *9*, 21–25.
- 57. Duarte, A. M. S.; van Mierlo, C. P. M.; Hemminga, M. A., *J. Phys. Chem. B* **2008**, *112*, 8664–8671.

# **Chapter 2 – Influence of Solution Composition on Gas-Phase Structure of Angiotensin I Determined by Ion Mobility Measurements**

#### Introduction

Angiotensin I (AGT I; Asp–Arg–Val–Tyr–Ile–His–Pro–Phe–His–Leu–OH) is an important intermediate peptide in the renin–angiotensin system<sup>1</sup> formed in the blood stream through the cleavage of the large precursor glycoprotein angiotensinogen by the enzyme renin. Although angiotensin I is biologically-inactive, it is quickly cleaved into the biologically-active octapeptide angiotensin II (AGT II; Asp–Arg–Val–Tyr–Ile–His–Pro–Phe–OH) by converting enzymes located on the luminal surfaces of endothelial cells.<sup>2</sup>

While the renin–angiotensin system is responsible for a variety of changes within the body, its ability to increase blood pressure leading to hypertension, heart failure and renal diseases has attracted considerable pharmaceutical interest.<sup>3, 4</sup> As a result, a significant amount of work has been done to elucidate the solution structure of angiotensin II, and its analogues, involving a variety of techniques including circular dichroism (CD),<sup>5-8</sup> nuclear magnetic resonance ( $^{1}$ H and  $^{13}$ C NMR),<sup>5-14</sup> IR and Raman spectroscopy,<sup>15, 16</sup> hydrogen–deuterium exchange (HDX)<sup>17</sup> and various conformational calculations.<sup>18-21</sup> These studies have produced a wide variety of proposed structures including  $\alpha$ -helices,<sup>22, 23</sup>  $\beta$ -pleated sheets, and both  $\beta$ - and  $\gamma$ -turns<sup>16, 24</sup> such that the number of proposed structures is likely disproportionate to the length of the peptide itself.<sup>14</sup>

Considerably less work has been done to elucidate the structure of the precursor angiotensin I. Although extensive studies have led to many conformational models for the smaller angiotensin II, few structures have been described for the larger precursor angiotensin I, and only recently was an experimentally determined structure reported.<sup>14</sup> However, as both peptides share a

common N-terminal and differ only in length and C-terminal configuration due to the presence or absence of the His<sup>9</sup>–Leu<sup>10</sup> dipeptide, it is likely that a large portion of the structure is preserved between the two peptides.<sup>14</sup>

Here, we use ion mobility spectrometry (IMS) techniques to examine the influence of solvent composition on the [M+3H]<sup>3+</sup> ion of angiotensin I produced by electrospray ionization (ESI).<sup>25</sup> Since the initial development of ESI as a "soft" ionization source for mass spectrometry (MS) a number of studies and experiments have been performed in an attempt to understand the structures of the solvent-free ions that are produced.<sup>26-36</sup> As an extension of these studies, it would be significant to be able to link the gas-phase structures of these ions with those of their solution-phase counterparts, which will allow the use of high-throughput gas-phase methods such as IMS to be used for rapid confirmation of proposed macromolecular structures derived from computational simulations.

The use of gas-phase methods for determining solution-phase structures requires an understanding of the relationship between the two states. McLafferty and co-workers were one of the first to illustrate the connection between gas-phase and solution-phase biomolecular conformation through hydrogen-deuterium ( $^{1}$ H/ $^{2}$ H) exchange experiments performed within a high-resolution Fourier-transform ion-cyclotron-resonance (FT–ICR) mass spectrometer. <sup>28</sup> In these experiments, they were able to infer structural information for gas-phase conformations of cytochrome c that corresponded to known conformations observed in solution. Further investigations by Jarrold and Clemmer have shown that it is possible to observe multiple partially-folded conformations of cytochrome c in the gas phase that are not observed with

nuclear magnetic resonance (NMR) or x-ray crystallography. Loo and co-workers have also shown that there is a link between the higher-order structures of gas- and solution-phase biomolecular ions.<sup>37</sup> Additionally, recent reports from Robinson, Bowers, and collaborators suggest that the gas-phase conformations of large non-covalent complexes may reflect those of their original solution-phase structures.<sup>38-40</sup> Finally, previous studies by Pierson and co-workers have shown that the number and relative abundance of solution states observed in ion mobility experiments is related to the original electrospray solution composition.<sup>41, 42</sup> In addition, these studies have illustrated the existence of a reproducible gas-phase quasi-equilibrium distribution of states for the triply-protonated state of bradykinin that is independent of the original solvent conditions. As this work is at a fairly early stage of development, it is important to develop it beyond a single system involving only a relatively small number of solution conditions.

Building upon these preliminary studies, two additional solvents — dimethyl sulfoxide and 2,2,2-trifluoroethanol — were selected due to their prevalence as NMR solvents and their tendency to favor the compact folding of angiotensin II analogs and derivatives. <sup>14, 16</sup> DMSO has also been used in previous NMR experiments with various angiotensin analogues to simulate non-polar receptor environments<sup>20, 43, 44</sup> and eliminate multiple conformational isomers. <sup>45</sup> Similarly, TFE has been extensively used as a co-solvent for the study of peptides due to its ability to stabilize some elements of the secondary structure, allowing the observation of  $\alpha$ -helices and  $\beta$ -sheets in NMR and CD studies. <sup>46-48</sup> Both TFE and DMSO have been identified as relatively useful membrane-mimetic organic solvents due to their aprotic nature, small relative dielectric constants, and large dipole moments (Table A.1). <sup>49</sup> However, DMSO is also known to

cause unfolding or denaturation of peptides above a certain concentration due to disruption of the intramolecular hydrogen bonds along the backbone.<sup>50</sup>

#### **Experimental Methods**

General

The general theory, <sup>51-56</sup> instrumentation, <sup>57-66</sup> and applicable techniques <sup>35, 54-56</sup> of IMS are described in detail elsewhere. For the purposes of this study, experiments were performed on a custom ion mobility spectrometer coupled to a time-of-flight (TOF) mass spectrometer (Figure 2.1) that was constructed in-house and described previously. <sup>57, 65, 66</sup> Positively charged ions of angiotensin I (acetate salt hydrate, ≥ 90% purity; Sigma, St. Louis, MO) were separately generated by ESI of 18 individual 0.01 mg·mL<sup>-1</sup> (~7.7 μM) solutions ranging from 0:100 to 90:10 (% volume) solvent:water under ambient laboratory conditions. Solutions were prepared by varying the proportion of water to solvent while maintaining a constant volume. In addition to high purity water (HPLC, EMD, Gibbstown, NJ), five organic solvents (all 99.9% purity, Sigma, St. Louis, MO) were employed without further purification: methanol, 1,4-dioxane, acetonitrile (ACN), 2,2,2-trifluoroethanol (TFE), and dimethyl sulfoxide (DMSO). Due to the aprotic nature of dioxane, ACN, and DMSO, no solutions greater than 90:10 (% volume) solvent:water were prepared.

Although only a brief explanation of the experimental procedure is included here, a more detailed description has been reported previously.<sup>41</sup> Ions are first collected and focused in a Smith-geometry hourglass ion funnel (F1)<sup>67, 68</sup> prior to injection into the drift tube through the use of a 150  $\mu$ s wide electrostatic gate (G1). The  $\sim$ 1.8 m drift tube (D1–D2) was filled with  $\sim$ 3.1 Torr He buffer gas at 300 K and operated with a uniform electric field of  $\sim$ 9.8 V·cm<sup>-1</sup>, such that

the ions separate based upon their individual mobilities. A second electrostatic ion funnel (F2) located in the middle of the drift tube radially focuses the diffuse ion packet as it travels through the drift tube. After further mobility separation in D2, the ions are radially focused again by a third ion funnel (F3) prior to exiting the drift tube. Upon exit, the ions pass through a differentially-pumped region and then orthogonally accelerated into a field-free TOF mass analyzer.

#### Selection and Activation.

In addition to the experiments performed using traditional IMS–MS, an important extension of this investigation involves the selection, activation and subsequent separation of specific ions of interest (IMS–IMS–MS). These types of experiments and the associated instrumentation have been detailed previously, <sup>41, 57, 65, 66</sup> but the basic technique may be described as follows.

Briefly, the two drift segments D1 and D2 are operated as independent drift tubes of 0.84 and 0.98 m, respectively. Ions are mobility selected as they pass through D1 via the application of a gating potential at G2. Consequently, a narrow packet of ions is transmitted through G2 by lowering the repulsive potential for 25–30 µs. Ions that enter this gate region prior to or after the application of the transmission pulse are neutralized by a Ni mesh grid (90% transmittance; Precision Eforming, Cortland, NY) attached to the first electrostatic lens of G2. The resulting mobility-selected ions are allowed to continue through F2 where they can be collisionally activated in the IA2 region prior to further mobility separation in D2.

The activation region IA2 is comprised of two electrostatic lenses separated by  $\sim 0.3$  cm. During experiments involving only selection, with no activation, the electric field between the two

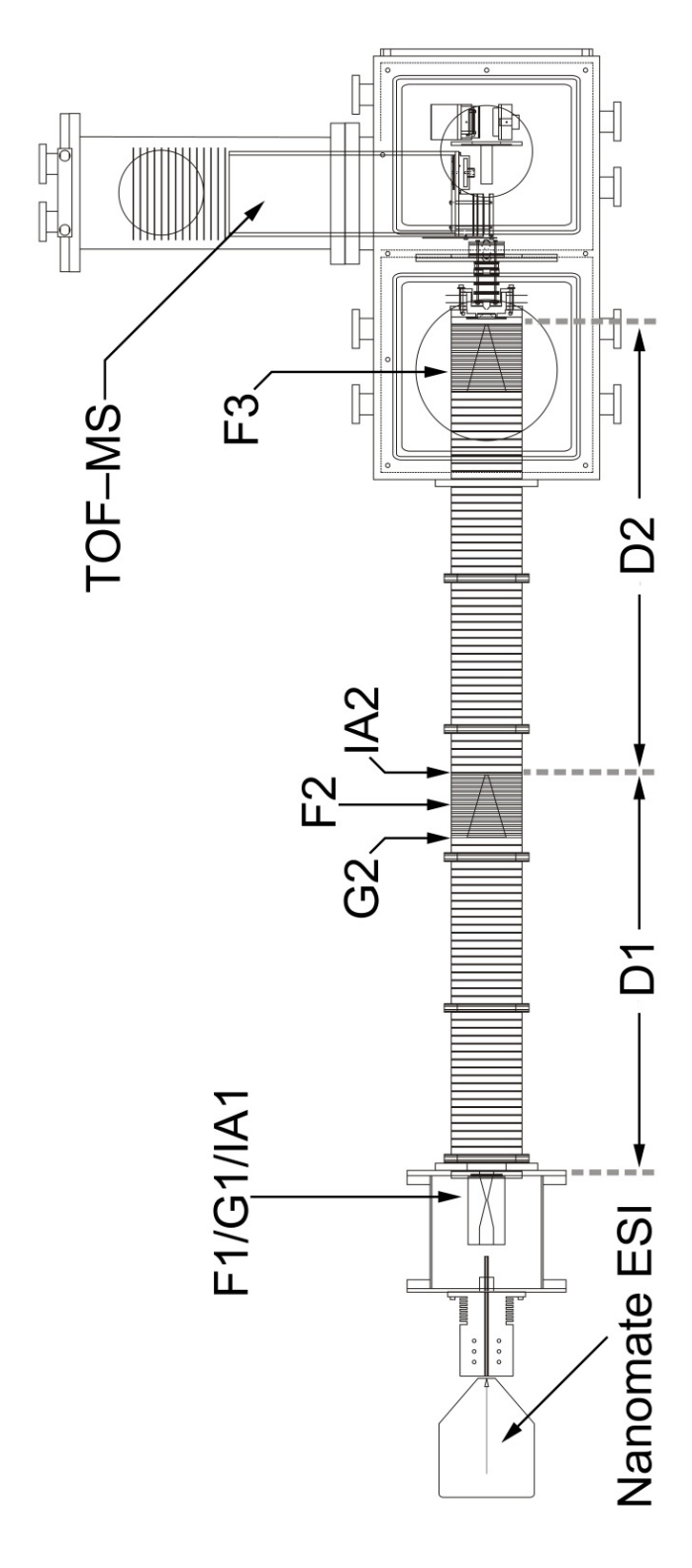


**Figure 2.1**: Schematic diagram of the IMS–IMS–MS instrument consisting of a robotic autosampler ESI source, a  $\sim$ 1.8 m drift tube (D1 and D2), and a time-of-flight mass spectrometer.

lenses is held equal to the applied DC field through F2. These initial field conditions result in an activation of 0 V, therefore ion activation is achieved by increasing this applied voltage above that of the surrounding field.

#### Calculating Collisional Cross-Sections.

A detailed method for calculating collisional cross-sections has been described previously,<sup>41</sup> so only a brief discussion of the method is included here. Under a uniform electric field, drift time distributions can be converted to a cross-section scale through the use of Eq. 2.1, where ze,  $k_b$ ,  $m_I$ , and  $m_B$  are the charge of the ion, Boltzmann's constant, the mass of the ion, and the mass of the buffer gas, respectively.<sup>53</sup>

$$\Omega = \frac{(18\pi)^{1/2}}{16} \frac{ze}{(k_B T)^{1/2}} \left[ \frac{1}{m_I} + \frac{1}{m_B} \right]^{1/2} \frac{t_d E}{L} \frac{760}{P} \frac{T}{273.2} \frac{1}{N}$$
(2.1)

Additionally,  $t_d$ , E, and L individually represent the drift time of the ion, the electric field strength and the drift length. The final three variables P, T, and N are correspondingly the pressure, temperature, and neutral number density (at STP) of the buffer gas. Drift time measurements for a given charge state can be converted into a collisional cross-section scale in order to assess the influence of the solvent on molecular conformation after correcting for differences in drift pressure and ambient temperature variations between experiments.

#### **Results and Discussion**

Solutions Containing Trifluoroethanol and Dimethyl Sulfoxide.

A representative two dimensional nested drift time(m/z) plot obtained upon electrospraying a solution of angiotensin I is shown in Figure 2.2. Features corresponding to three main ions are observed. The [M+2H]<sup>2+</sup> ion is observed at a drift time of ~19.1 ms, with a m/z value of 648.3

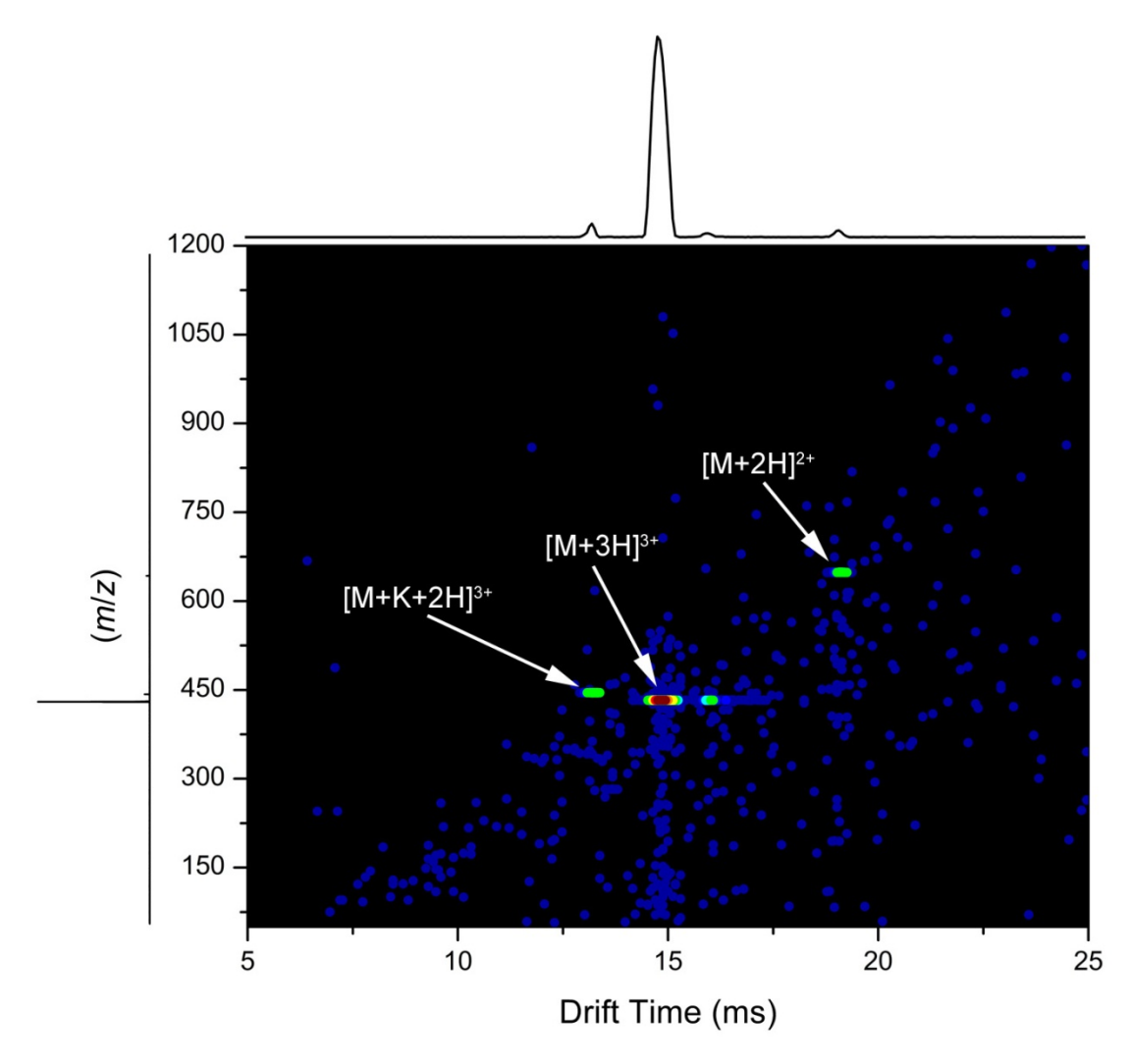


**Figure 2.2**: Two dimensional plot representing nested m/z measurements within drift time measurements for angiotensin I in a 50:50 methanol:water solution. Compressions of each dimension are shown on the x- and y-axes, representing total ion drift time distribution and mass spectrum, respectively. The pressure of the He buffer gas was maintained at  $\sim 3.10$  Torr at 300 K.

Th. Although the  $[M+3H]^{3+}$  ion, with a measured drift time of ~14.8 ms, dominates the spectrum, another feature representing a triply-charged species is observed at lower drift times (~13.2 ms). This feature has been assigned as the  $[M+K+2H]^{3+}$  ion. Furthermore, a small population representing a partially elongated conformation of the  $[M+3H]^{3+}$  ion is also observed at ~16 ms.

From two-dimensional datasets such as that shown in Figure 2.2, drift time distributions of individual ions can be obtained by integrating all intensities across a narrow m/z range centered about the ion of interest. The generation of these extracted spectra from different experiments employing different solvents provides information about the different conformations that are present in solution. Drift slices representing the triply-protonated species of angiotensin I in solutions of trifluoroethanol are shown on a drift time scale as a function of solvent composition (Figure 2.3A). Increasing the relative concentration of TFE produces no significant additional features. As mentioned previously, one feature corresponding to the [M+3H]<sup>3+</sup> ion is observed at ~14 ms with a peak width of 0.66 ms. At low concentrations (< 50% TFE), this peak remains relatively broad (FWHM  $\sim$ 0.6–0.9 ms). However, at concentrations  $\geq$  50% TFE, the distribution becomes much narrower as the width of the peak decreases (~0.4 ms). Additional poorly resolved partially-elongated features are also observed at higher TFE concentrations with drift times ranging from 14.8–17.0 ms. These partially-elongated conformations are not present in any significant abundance at concentrations less than 60% TFE, although trace amounts can be observed.

The peak sharpening observed in Figure 2.3A suggests that either less conformational transformation occurs during the IMS measurement or that fewer structures of different sizes result from the "freezing out" of solution-phase structures as the concentration of TFE is increased. Possible mechanisms for explaining why polyfluorinated alcohols such as TFE and 1,1,1,3,3,3-hexafluoroisopropanol (HFIP) affect peptide structure include the enhancement of intrapeptide hydrogen bonding and a lessening of the hydrophobic effect. TFE is known to be a stronger hydrogen bond donor than water, and preferentially binds to the backbone carbonyl oxygen leading to enhanced intrapeptide hydrogen bonding often resulting in increased stabilization of helical structures. The favoring of specific structures in solution could account for the decreased peak widths observed for gas-phase species at higher concentrations of TFE.

Extracted drift profiles of the triply protonated species of angiotensin I from solutions containing varying amounts of DMSO reveal a markedly different behavior for the formation of gas-phase conformers. As shown in Figure 2.3B, the introduction of a relatively small amount of DMSO (5% by volume) results in the formation of two additional partially-elongated conformations. Initially, at concentrations of DMSO that are less than  $\sim$ 20%, each of the observed peaks is relatively broad (FWHM = 0.66–0.78 ms). The feature representing the most compact (highest mobility) conformation centered at  $\sim$ 14.7 ms begins to narrow at 25% DMSO, ultimately reducing in width by  $\sim$ 0.50 ms at the highest concentration. Two partially-elongated conformations are observed at  $\sim$ 15.9 and  $\sim$ 16.9 ms, respectively. These two features are relatively broad peaks at low concentrations of DMSO (< 30%); however, they both experience a decrease in peak width as the concentration of DMSO is increased. At high DMSO concentrations a decrease of  $\sim$ 0.4 ms in the FWHM was observed for the low mobility features.

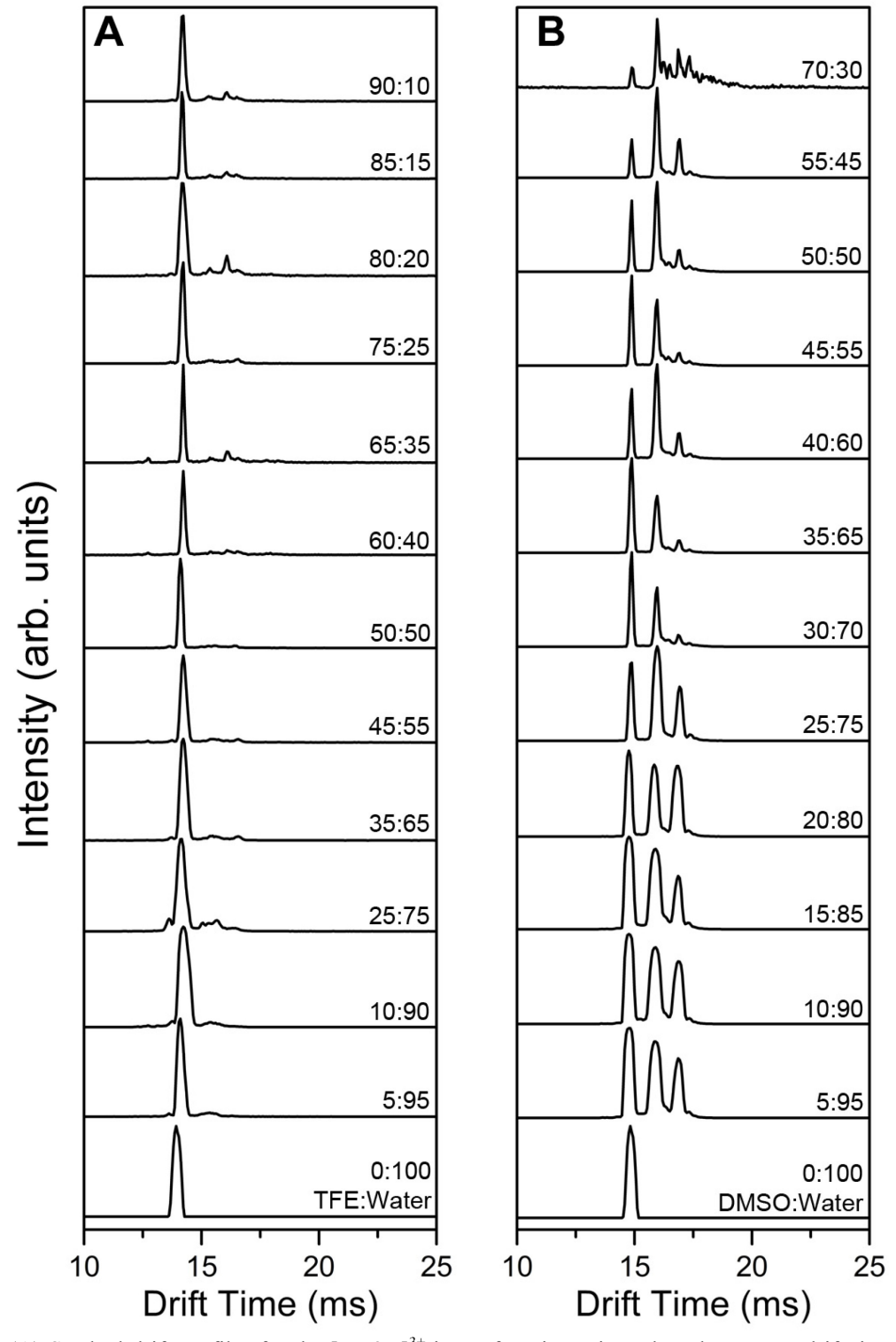


**Figure 2.3**: (**A**) Stacked drift profiles for the  $[M+3H]^{3+}$  ions of angiotensin I plotted on a raw drift time scale as a function of increasing concentration of TFE from pure water solutions up to 90% (by volume) TFE. (**B**) Stacked drift profiles for the  $[M+3H]^{3+}$  ions of angiotensin I plotted on a drift time scale as a function of increasing concentration of DMSO from pure water solutions up to 70% (by volume) DMSO. For all experiments represented in the figure the He buffer gas was maintained at a pressure of ~3.5 Torr.

The three conformations of the angiotensin I [M+3H]<sup>3+</sup> ion are initially well represented upon direct electrospray of the DMSO solutions, resulting in relatively intense broad peaks. However, as the concentration of DMSO is increased, the shape and relative intensity of each of the three features changes. First, the peak representing the most compact form begins to narrow, again possibly as a result of the favoring of a specific conformer type, suggesting a stabilization of the structure prior to the ionization process analogous to the proposed mechanism for solutions containing trifluoroethanol. This peak narrowing is then later observed at higher quantities of DMSO for the two partially elongated conformations, suggesting that it may require a greater amount of DMSO to favor (or disfavor) other closely related solution structures. As the concentration of DMSO is increased beyond ~25% by volume, some of the initially large features begin to diminish in intensity. The [M+3H]<sup>3+</sup> ion is only observable by electrospraying solutions up to ~70% DMSO by volume. At concentrations greater than 70% DMSO, no features corresponding to any of the ionized species of angiotensin I are observed. This reduction in signal for the peptide ions is largely a result of preferential ionization of the solvent molecules themselves as well as the formation of solvent adducts. As the concentration of DMSO increases, the signal for the [DMSO+H]<sup>+</sup> and [2 DMSO+H]<sup>+</sup> ions also increases, ultimately becoming the only observable features in the spectrum.

A recent study by Sterling and co-workers has demonstrated that DMSO can be used as a supercharging reagent for protein ions formed by electrospray.<sup>69</sup> In their experiments with hen egg white lysozyme and equine myoglobin (~14.3 and 16.9 kDa, respectively), increasing the concentration of DMSO resulted in a shift toward the formation of ions with higher charge states. To a certain extent, a similar effect is observed in the much smaller angiotensin I (~1.3 kDa) as

the addition of only a small amount of DMSO results in a significant favoring of the production of the 3+ charge state. Higher charge states ( $\geq 4+$ ) are not observed for angiotensin I, likely as a result of the full protonation of the available basic residues on the peptide and the resulting Coulombic repulsion preventing the incorporation of additional charge on the molecule.

Dimethyl sulfoxide is useful as a supercharging agent for MS studies because it acts as a denaturant for peptides and proteins, resulting in significant changes in the structure of the molecule, and increasing the number of accessible charge sites. For small peptides such as angiotensin I, the addition of even 5% DMSO by volume results in new solution structures represented by a partially elongated structural population in the gas phase. It is possible that larger peptides and proteins would exhibit similar elongated structures due to denaturation. For these larger species, an even greater number of different conformation types might be accessible.

Conformational Changes Observed Upon Activation in DMSO.

Although the formation of multiple conformations in solutions containing DMSO may complicate solution-phase structural studies, the result introduces a new paradigm regarding the concept of the "native" state of biological molecules. One explanation of the results observed in Figure 2.4 is that multiple structural types are present in solutions containing DMSO and that solution composition dictates favored conformations.

Although dioxane-containing solutions also produce additional elongated gas-phase distributions, their intensity is significantly reduced compared to those observed in solutions of DMSO. Solutions containing DMSO produce three narrow distributions that are not observed in other solvents (Figure 2.4). Consequently we investigate DMSO-containing solvent systems

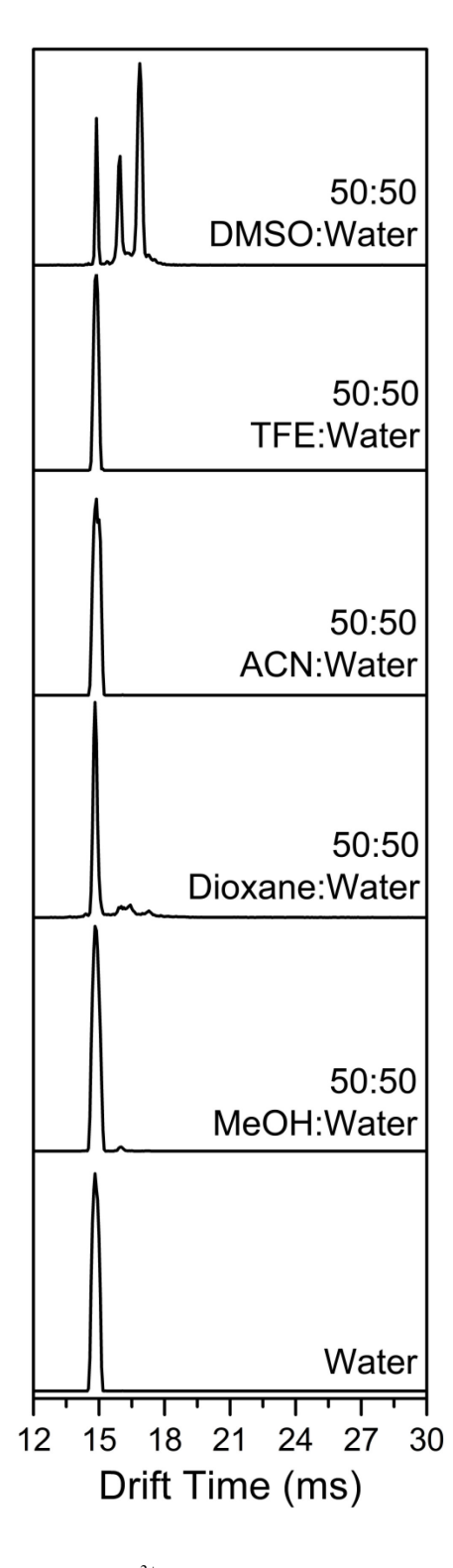


**Figure 2.4**: Stacked drift profiles for the  $[M+3H]^{3+}$  ion of angiotensin I plotted on a drift time scale as a function of solvent composition. Here, the influence of each solvent is compared directly for 50:50 (% volume) mixtures of solvent and water. For all experiments represented in the figure the He buffer gas was maintained at a pressure of  $\sim$ 3.5 Torr.

here, although significant work involving the influence of dioxane-containing solutions on other peptide systems has been reported elsewhere.<sup>42</sup>

A number of studies have been carried out to determine the relative stability of the three gasphase conformers of angiotensin I obtained from the DMSO solutions. Drift time distributions for the [M+3H]<sup>3+</sup> ion of angiotensin I were collected for the 25:75 (% volume) DMSO:water mixture. At higher relative concentrations, DMSO is competitively ionized alongside the target analyte resulting in an overall decrease in desired ion signal and an increase in the population of singly protonated DMSO monomers and dimers.

Upon selection of the highest mobility ion (conformer A), a narrow distribution is obtained. The subsequent increase in activation energy from 0 V to 25 V results in no additional changes to the distribution of conformer A as shown in Figure 2.5. As the activation voltage is sequentially increased up to 175 V, conformer A remains stable and no changes are observed until fragmentation of the peptide occurs at applied activation voltages greater than 150 V. Similarly, selection of conformer B without activation results in another narrow distribution, but with a slight amount (~4% relative abundance) converting into the smaller conformer A (Figure 2.5). As the activation voltage is increased from 0 to 25 V, both conformers A and B are clearly present in large abundance (~42 and 58% relative abundance, respectively). A further increase in the activation energy to 50 V results in a complete conversion of conformer B into conformer A. Similarly, the increased stability for the newly formed conformer A is observed as the activation voltage is increased up to ~150 V, beyond which fragmentation of the peptide occurs as previously mentioned.

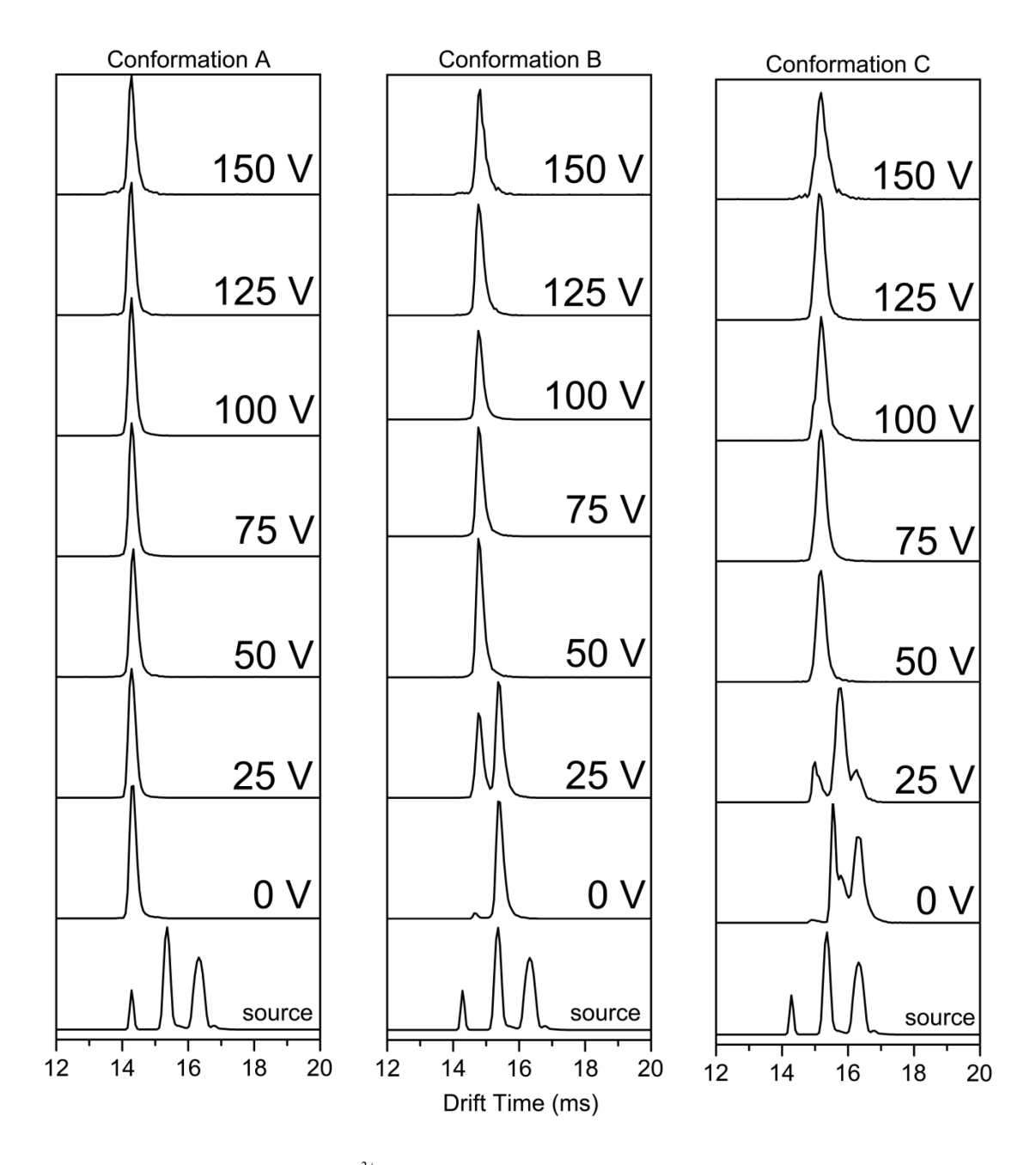


**Figure 2.5**: Drift profiles of the  $[M+3H]^{3+}$  angiotensin I ion plotted on a drift time scale. The bottom curve in each panel shows the ESI source distribution obtained for the 25:75 (% volume) DMSO:water. The individual panels (arbitrarily assigned A through C) show one of three separate experiments beginning with the initial selection of a conformation with no activation followed by successively increasing activation voltages up to 150 V. Activation voltages greater than 150 V result in subsequent fragmentation of the target ion and are therefore omitted. For all experiments the He buffer gas was maintained at a pressure of  $\sim$ 3.0 Torr. Selections of the three conformers A through C all converge to the same distribution of the stable conformer A at an activation voltage of 50 V.

Selection of conformer C without activation produces two poorly-resolved features representing conformers B and C (58 and 41% relative abundance, respectively) and a trace amount of conformer A (~1% relative abundance). Unlike conformers A and B which can both be cleanly selected at G2 resulting in narrow distributions, conformer C is relatively unstable and begins to immediately transform into the more compact structures upon the addition of even the smallest amount of energy (Figure 2.5). Here, despite a lack of applied activation energy, structural transformations resulting from energetically-increased collisions with the buffer gas are observed. Although we do not measure additional collisional energy during selection, the electrostatic gate (G2) does impart a slight acceleration to the ions as they near the end of D1. For stable gas-phase structures such as conformers A and B, this minute increase in collisional energy as a result of the increased electric field surrounding G1 has little to no effect, but for unstable conformations that may only be stabilized by residual solvent molecules, the additional collisional energy that is imparted upon the ion may be enough to cause conformational changes. As the activation voltage is increased to 25 V, the population distribution begins to favor the smaller conformers A and B (~22, 61 and 17% relative abundance, respectively). As with conformer B, application of activation voltages greater than 50 V result in complete conversion to conformer A and fragmentation of the peptide occurs above 150 V.

This conversion from the two elongated states (B and C) into the more compact and stable conformer A serves to illustrate an interesting phenomenon. As described earlier, a significant amount of recent experimental work has been done in an attempt to link solution and gas-phase structures. In certain cases, such as those shown previously with bradykinin, <sup>41, 42</sup> a stable quasi-equilibrium of states exists in the gas phase that can be accessed by selection and activation of

any observable state. Similarly, in this case, a gas-phase distribution consisting of multiple conformers exists. However, as shown with angiotensin I and DMSO, only one stable gas-phase population persists upon collisional heating suggesting that a quasi-equilibrium of states does not exist for this system. Nonetheless, the conversion of the B and C states into the more compact A state suggests that these two partially-elongated states may be related, stable solution-phase structures. It is worth noting that the A state, which is observed in all of the solution conditions investigated, is stable in both the solution- and gas-phases. The relatively low energies required to convert the B and C states into the stable A state suggests that these elongated forms may have retained elements of their original solution structure even after the transition into the gas phase.

### Implications of DMSO and TFE as Solvents

Dimethyl sulfoxide and trifluoroethanol produce dramatically different gas-phase distributions of angiotensin I ions. Solutions of DMSO appear to favor multiple solution conformations that can be observed in the gas phase. This multiplicity of conformers does not appear to be common for other solvents such as methanol or acetonitrile, but is seen to some degree in solutions of 1,4-dioxane. It is worthwhile to note that DMSO, or more commonly its deuterated form DMSO– $d_6$ , is often used as an NMR solvent when probing the structure of proteins and peptides. The results here suggest that this may be problematic as the use of DMSO results in the formation of several structures of angiotensin I. Such conditions could result in some uncertainty in solution-phase NMR measurements.

It is instructional to consider the chemical properties of the solvent systems. DMSO is a strong hydrogen bond acceptor.<sup>50, 72</sup> Conversely, trifluoroethanol is a strong hydrogen bond donor<sup>45</sup> resulting in the stabilization of intramolecular hydrogen bonds. In this case, the use of TFE as an

NMR solvent may reduce the uncertainty in the structural measurements. However, this stabilization of the peptide structure also results in a decreased ability to measure dynamic changes in the conformations that may be useful for structure-function relationship studies. Thus, it becomes necessary to choose solvents carefully in order to match their specific peptide-interaction characteristics with the goals of the experiment.

#### **Conclusions**

Ion mobility measurements of the angiotensin I [M+3H]<sup>3+</sup> ion formed by direct ESI show evidence for multiple stable solution-phase structures in solutions of DMSO. These solution-phase structures are observed as three distinct gas-phase conformers that are quickly reduced to a single stable gas-phase distribution upon low energy activation in multidimensional IMS-IMS-MS experiments. The observance of these temporarily stable elongated forms in the gas phase, and their convergence to a single stable gas-phase distribution, suggests that certain elements of solution-phase structures are retained during the transition into the gas phase. While this result does not definitively illustrate the connection between gas-phase conformations and their solution-phase antecedents, it does suggest that some of the solvent-stabilized structures are retained in the gas phase to a certain degree and can therefore be observed and studied using these higher-throughput methods.

# Acknowledgements

This work is supported in part by the Indiana University METAcyte initiative, which receives funding from grants provided by the Lilly Endowment.

# References

- 1. Page, I. H.; Bumpus, F. M., *Physiol. Rev.* **1961**, *41*, 331–390.
- 2. Reid, I. A., Arch. Intern. Med. 1985, 145, 1475–1479.
- 3. Regoli, D.; Park, W. K.; Rioux, F., *Pharmacol. Rev.* **1974**, *26*, 69–123.
- 4. Moore, G. J.; Matsoukas, J. M., *Biosci. Rep.* **1985**, *5*, 407–416.
- 5. Fermandjian, S.; Sakarellos, C.; Piriou, F.; Juy, M.; Toma, F.; Thanh, H. L.; Lintner, K.; Khosla, M. C.; Smeby, R. R.; Bumpus, F. M., *Biopolymers* **1983**, *22*, 227–231.
- 6. Fermandjian, S.; Piriou, F.; Sakarellos, C.; Lintner, K.; Khosla, M. C.; Smeby, R. R.; Bumpus, F. M., *Biopolymers* **1981**, *20*, 1971–1983.
- 7. Aumelas, A.; Sakarellos, C.; Lintner, K.; Fermandjian, S.; Khosla, M. C.; Smeby, R. R.; Bumpus, F. M., *Proc. Natl. Acad. Sci. U. S. A.* **1985**, *82*, 1881–1885.
- 8. Khosla, M. C.; Stachowiak, K.; Smeby, R. R.; Bumpus, F. M.; Piriou, F.; Lintner, K.; Fermandjian, S., *Proc. Natl. Acad. Sci. U. S. A.* **1981**, *78*, 757–760.
- 9. Matsoukas, J. M.; Moore, G. J., Arch. Biochem. Biophys. 1986, 248, 419–423.
- 10. Matsoukas, J. M.; Bigam, G.; Zhou, N.; Moore, G. J., *Peptides* **1990**, *11*, 359–366.
- 11. Galardy, R. E.; Liakopoulou-Kyriakides, M., Int. J. Pept. Protein Res. 1982, 20, 144–148.
- 12. Lenkinski, R. E.; Stephens, R. L., J. Inorg. Biochem. 1983, 18, 175–180.
- 13. Deslauriers, R.; Paiva, A. C. M.; Schaumburg, K.; Smith, I. C. P., *Biochemistry* **1975**, *14*, 878–886.
- 14. Spyroulias, G. A.; Nikolakopoulou, P.; Tzakos, A.; Gerothanassis, I. P.; Magafa, V.; Manessi Zoupa, E.; Cordopatis, P., *Eur. J. Biochem.* **2003**, *270*, 2163–2173.

- 15. Sakarellos, C.; Lintner, K.; Piriou, F.; Fermandjian, S., *Biopolymers* **1983**, *22*, 663–687.
- 16. Fermandjian, S.; Fromageot, P.; Tistchenko, A.-M.; Leicknam, J.-P.; Lutz, M., *Eur. J. Biochem.* **1972**, *28*, 174–182.
- 17. Lenkinski, R. E.; Stephens, R. L.; Krishna, N. R., *Biochemistry* **1981**, *20*, 3122–3126.
- 18. De Coen, J.-L.; Ralston, E., *Biopolymers* **1977**, *16*, 1929–1943.
- 19. Rauk, A.; Hamilton, G.; Moore, G. J., *Biochem. Biophys. Res. Commun.* **1987**, *145*, 1349–1355.
- 20. Joseph, M. P.; Maigret, B.; Scheraga, H. A., Int. J. Pept. Protein Res. 1995, 46, 514–526.
- 21. Preto, M. A. C.; Melo, A.; Maia, H. L. S.; Mavromoustakos, T.; Ramos, M. J., *J. Phys. Chem. B* **2005**, *109*, 17743–17751.
- 22. Krimm, S.; Bandekar, J., Adv. Protein Chem. 1986, 38, 181–364.
- 23. Byler, D. M.; Susi, H., *Biopolymers* **1986**, *25*, 469–487.
- 24. Printz, M. P.; Bleich, H.; Nemethy, G., *Nature-New Biology* **1972**, *237*, 135–140.
- 25. Fenn, J. B.; Mann, M.; Meng, C. K.; Wong, S. F.; Whitehouse, C. M., *Science* **1989**, *246*, 64–71.
- 26. Chowdhury, S. K.; Chait, B. T., Biochem. Biophys. Res. Commun. 1990, 173, 927–931.
- 27. Katta, V.; Chait, B. T., *Rapid Commun. Mass Spectrom.* **1991**, *5*, 214–217.
- Suckau, D.; Shi, Y.; Beu, S. C.; Senko, M. W.; Quinn, J. P.; Wampler, F. M.;
   McLafferty, F. W., *Proc. Natl. Acad. Sci. U. S. A.* 1993, 90, 790–793.
- 29. Covey, T.; Douglas, D. J., J. Am. Soc. Mass Spectrom. 1993, 4, 616–623.
- 30. Clemmer, D. E.; Hudgins, R. R.; Jarrold, M. F., *J. Am. Chem. Soc.* **1995**, *117*, 10141–10142.

- 31. Vonhelden, G.; Wyttenbach, T.; Bowers, M. T., Science 1995, 267, 1483–1485.
- 32. Bowers, M. T.; Marshall, A. G.; McLafferty, F. W., J. Phys. Chem. 1996, 100, 12897–12910.
- 33. Smith, R. D.; Bruce, J. E.; Wu, Q. Y.; Lei, Q. P., Chem. Soc. Rev. 1997, 26, 191–202.
- 34. Williams, E. R., J. Mass Spectrom. **1996**, 31, 831–842.
- 35. Hoaglund-Hyzer, C. S.; Counterman, A. E.; Clemmer, D. E., *Chem. Rev.* **1999**, *99*, 3037–3079.
- 36. Wyttenbach, T.; Bowers, M. T., Annu. Rev. Phys. Chem. 2007, 58, 511–533.
- 37. Loo, J. A.; He, J. X.; Cody, W. L., J. Am. Chem. Soc. 1998, 120, 4542–4543.
- 38. Ruotolo, B. T.; Giles, K.; Campuzano, I.; Sandercock, A. M.; Bateman, R. H.; Robinson, C. V., *Science* **2005**, *310*, 1658–1661.
- 39. Painter, A. J.; Jaya, N.; Basha, E.; Vierling, E.; Robinson, C. V.; Benesch, J. L. P., *Chem. Biol.* **2008**, *15*, 246–253.
- 40. Bernstein, S. L.; Dupuis, N. F.; Lazo, N. D.; Wyttenbach, T.; Condron, M. M.; Bitan, G.; Teplow, D. B.; Shea, J.-E.; Ruotolo, B. T.; Robinson, C. V.; Bowers, M. T., *Nat. Chem.* **2009**, *1*, 326–331.
- 41. Pierson, N. A.; Valentine, S. J.; Clemmer, D. E., J. Phys. Chem. B **2010**, 114, 7777–7783.
- 42. Pierson, N. A.; Chen, L.; Valentine, S. J.; Russell, D. H.; Clemmer, D. E., *J. Am. Chem. Soc.* **2011**, *133*, 13810–13813.
- 43. Matsoukas, J. M.; Hondrelis, J.; Keramida, M.; Mavromoustakos, T.; Makriyannis, A.; Yamdagni, R.; Wu, Q.; Moore, G. J., *J. Biol. Chem.* **1994**, *269*, 5303–5312.
- 44. Cordopatis, P.; Manessizoupa, E.; Theodoropoulos, D.; Bosse, R.; Bouley, R.; Gagnon, S.; Escher, E., *Int. J. Pept. Protein Res.* **1994**, *44*, 320–324.

- 45. Buck, M., Q. Rev. Biophys. 1998, 31, 297–355.
- 46. Hong, D.-P.; Hoshino, M.; Kuboi, R.; Goto, Y., J. Am. Chem. Soc. 1999, 121, 8427–8433.
- 47. Jasanoff, A.; Fersht, A. R., *Biochemistry* **1994**, *33*, 2129–2135.
- 48. Roccatano, D.; Colombo, G.; Fioroni, M.; Mark, A. E., *Proc. Natl. Acad. Sci. U. S. A.* **2002**, *99*, 12179–12184.
- 49. Chatterjee, A.; Bothra, A. K., *Int. J. Integ. Biol.* **2010**, *9*, 21–25.
- 50. Duarte, A. M. S.; van Mierlo, C. P. M.; Hemminga, M. A., *J. Phys. Chem. B* **2008**, *112*, 8664–8671.
- 51. Mack, E., J. Am. Chem. Soc. 1925, 47, 2468–2482.
- 52. Revercomb, H. E.; Mason, E. A., *Anal. Chem.* **1975**, *47*, 970–983.
- 53. Mason, E.; McDaniel, E., *Transport Properties of Ions in Gases*. Wiley: New York, 1988.
- 54. Shvartsburg, A. A.; Jarrold, M. F., Chem. Phys. Lett. 1996, 261, 8691.
- 55. Mesleh, M. F.; Hunter, J. M.; Shvartsburg, A. A.; Schatz, G. C.; Jarrold, M. F., *J. Phys. Chem.* **1996**, *100*, 16082–16086.
- 56. Wyttenbach, T.; Helden, G. v.; Batka, J. J. J.; Carlat, D.; Bowers, M. T., *J. Am. Soc. Mass Spectrom.* **1997**, *8*, 275–282.
- 57. Koeniger, S. L.; Merenbloom, S. I.; Clemmer, D. E., *J. Phys. Chem. B* **2006**, *110*, 7017–7021.
- 58. Wittmer, D.; Chen, Y. H.; Luckenbill, B. K.; Hill, H. H., *Anal. Chem.* **1994**, *66*, 2348–2355.

- Gillig, K. J.; Ruotolo, B.; Stone, E. G.; Russell, D. H.; Fuhrer, K.; Gonin, M.; Schultz, A. J., Anal. Chem. 2000, 72, 3965–3971.
- 60. Hoaglund, C. S.; Valentine, S. J.; Sporleder, C. R.; Reilly, J. P.; Clemmer, D. E., *Anal. Chem.* **1998**, *70*, 2236–2242.
- 61. Hoaglund-Hyzer, C. S.; Li, J.; Clemmer, D. E., Anal. Chem. 2000, 72, 2737–2740.
- 62. Valentine, S. J.; Kulchania, M.; Barnes, C. A. S.; Clemmer, D. E., *Int. J. Mass. Spectrom.* **2001**, *212*, 97–109.
- 63. Tang, K.; Shvartsburg, A. A.; Lee, H.-N.; Prior, D. C.; Buschbach, M. A.; Li, F.; Tolmachev, A. V.; Anderson, G. A.; Smith, R. D., *Anal. Chem.* **2005**, *77*, 3330–3339.
- Koeniger, S. L.; Merenbloom, S. I.; Valentine, S. J.; Jarrold, M. F.; Udseth, H. R.; Smith,
   R. D.; Clemmer, D. E., *Anal. Chem.* 2006, 78, 4161–4174.
- 65. Merenbloom, S. I.; Koeniger, S. L.; Valentine, S. J.; Plasencia, M. D.; Clemmer, D. E., *Anal. Chem.* **2006**, *78*, 2802–2809.
- 66. Counterman, A. E.; Valentine, S. J.; Srebalus, C. A.; Henderson, S. C.; Hoaglund, C. S.; Clemmer, D. E., *J. Am. Soc. Mass Spectrom.* **1998**, *9*, 743–759.
- 67. Shaffer, S. A.; Tang, K.; Anderson, G. A.; Prior, D. C.; Udseth, H. R.; Smith, R. D., *Rapid Commun. Mass Spectrom.* **1997**, *11*, 1813–1817.
- 68. Shaffer, S. A.; Prior, D. C.; Anderson, G. A.; Udseth, H. R.; Smith, R. D., *Anal. Chem.* **1998**, 70, 4111–4119.
- 69. Sterling, H.; Prell, J.; Cassou, C.; Williams, E., *J. Am. Soc. Mass Spectrom.* **2011**, *22*, 1178–1186.
- 70. Garbay-Jaureguiberry, C.; Roques, B. P.; Oberlin, R.; Anteunis, M.; Lala, A. K., *Biochem. Biophys. Res. Commun.* **1976**, *71*, 558–565.

- 71. Levian-Teitelbaum, D.; Kolodny, N.; Chorev, M.; Selinger, Z.; Gilon, C., *Biopolymers* **1989**, *28*, 51–64.
- 72. McGarry, P. F.; Jockusch, S.; Fujiwara, Y.; Kaprinidis, N. A.; Turro, N. J., *J. Phys. Chem. A* **1997**, *101*, 764–767.

# Chapter 3 – Aggregation of Angiotensin II Monitored in Real Time by Ion Mobility Spectrometry

#### Introduction

The study of protein and peptide aggregation in biological systems has gained increased consideration as a result of the role of oligomers and fibrils in the development of neurodegenerative disorders including Parkinson's and Alzheimer's diseases.<sup>1, 2</sup> It is known that even small protein oligomers can cause irreversible neuronal injuries, and the mechanism associated with the self-assembly of these proteins is still a matter of debate.<sup>3</sup> Recently, it has been shown that many generic proteins or peptides can form ordered aggregates under suitable conditions, though these conditions may vary slightly for individual molecules.<sup>4</sup> The relationship among the structures of the polypeptides, the surrounding environment, and the formation of aggregation products is relatively difficult to study in the solution phase due to the rapid interconversion of structural conformers. The use of gas-phase techniques removes some of these complications, where the transition of molecules from the solution phase into the gas phase during the electrospray ionization (ESI)<sup>5</sup> process rapidly removes surrounding solvent molecules, resulting in stabilization of specific structures, and an overall reduction in structural interconversion. Thus, an understanding of the structure of aggregate ions in the gas-phase may provide clues to antecedent solution conformations, aiding in the elucidation of aggregation mechanisms.

Previous experimental results have shown that ion mobility experiments can be used to separate multimeric ions that are often buried within mass spectrometry data.<sup>7</sup> In early experiments, mass spectra associated with bradykinin would often show three main features corresponding to the  $[M+H]^+$ ,  $[M+2H]^{2+}$ , and  $[M+3H]^{3+}$  ions. However, upon the introduction of mobility separation

prior to mass analysis, it became possible to easily separate and identify four distinct features with the same m/z previously assigned as the  $[M+H]^+$  species by mass spectrometry (MS) alone.<sup>7</sup> By carefully extracting the mass spectra for each of the mobility resolved features, and analyzing the isotopic distribution it becomes possible to assign specific oligomeric identities to each of the peaks in the drift profile.

In this study we expand on this previous work and examine the aggregation patterns of the octapeptide angiotensin II (Asp–Arg–Val–Tyr–Ile–His–Pro–Phe–OH) over time with ion mobility spectrometry and mass spectrometry (IMS–MS). Preliminary work has shown that the aggregation of angiotensin II is influenced by the solvent composition and that polyfluorinated alcohols can be used to enhance the formation of the [M+H]<sup>+</sup> ion. These polyfluorinated alcohols can also be used to dissociate residual aggregates remaining from the manufacturing and purification processes as well, allowing the subsequent formation of dimers and trimers to be monitored over time.

Early studies on the aggregation potential of angiotensin II were inconclusive, and suggest that the peptide was capable of forming dimers at most.<sup>8</sup> Further structural investigation of the peptide was performed with both <sup>1</sup>H and <sup>13</sup>C nuclear magnetic resonance (NMR), neither of which saw significant evidence for the presence of dimers or higher order aggregates.<sup>9, 10</sup> Circular dichroism (CD) and intermolecular nuclear Overhauser effect (NOE) experiments have also noticed a distinct lack of aggregate species in solutions containing ethanol and trifluoroethanol.<sup>11, 12</sup> Gel electrophoresis is often the preferred method for the analysis of both simple and complex peptide mixtures;<sup>13</sup> however, the use of detergents such as sodium dodecyl

sulfate (SDS) often results in the loss of native structural conformations.<sup>14</sup> Furthermore, in order to study the formation of aggregation over time, aliquots of an incubating sample must be collected at various time points and frozen in order to slow or stop the aggregation process until a sufficient number of samples have been collected for analysis, introducing a certain amount of error, and delaying the results. Thus, we use ion mobility spectrometry and mass spectrometry in order to overcome some of these aforementioned difficulties by avoiding denaturing solvents to preserve elements of the native structure and monitoring the formation of aggregates in near real time.

# **Experimental**

General

The general theory, <sup>15-20</sup> instrumentation, <sup>7, 21-29</sup> and technical application <sup>18-20, 30</sup> of IMS are described in detail elsewhere. For the purposes of this study, experiments were performed on an ion mobility spectrometer coupled to a time-of-flight (TOF) mass spectrometer (Figure 3.1) that was constructed in-house as previously described. <sup>7, 21, 28</sup> Briefly, electrosprayed angiotensin II ions are first collected and focused in a Smith-geometry (hour glass) ion funnel (F1)<sup>31, 32</sup> prior to injection into a drift tube using a 150 μs wide electrostatic gate (G1). The ~1.8 m drift tube (D1–D2) is filled with ~3.1 Torr He buffer gas at 300 K and operated with a uniform electric field of ~9.8 V·cm<sup>-1</sup> such that the ions separate based upon their individual mobilities. A second ion funnel (F2) located in the middle of the drift tube radially focuses the diffuse ion packet as it travels through the drift tube. After further mobility separation in D2, the ions are radially focused again by a third ion funnel (F3) prior to exiting the drift tube. Upon exiting, the ions pass through a differentially-pumped region and then are orthogonally accelerated into a field-free TOF mass analyzer.

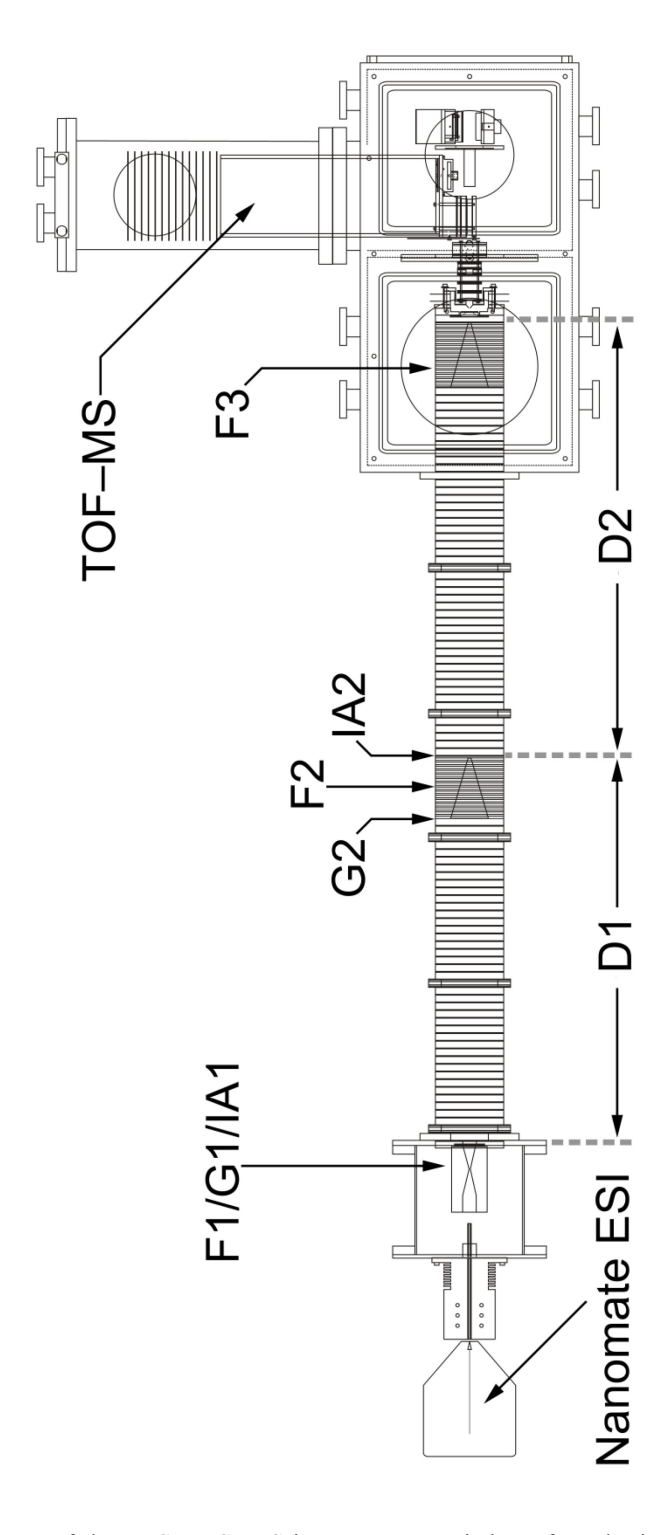


Figure 3.1: Schematic diagram of the IMS–IMS–MS instrument consisting of a robotic autosampler ESI source, a  $\sim$ 1.8 m drift tube (D1 and D2), and a time-of-flight mass spectrometer.

# ESI Solution Conditions

Positively charged ions of angiotensin II (trifluoroacetate salt hydrate, ≥ 98% purity; EMD, Gibbstown, NJ) were generated by ESI of individual 1.0 mg·mL<sup>-1</sup> (~0.96 mM) solutions in 50:50 (%volume) 2,2,2-trifluoroethanol:water and 50:50 (% volume) acetonitrile:water. Trifluoroethanol (TFE; ≥ 99.0%, Sigma, St. Louis, MO), acetonitrile (ACN; ≥99.9%, Sigma, St. Louis, MO), and high purity water (HPLC, EMD, Gibbstown, NJ) were used without additional purification. To dissociate preformed aggregation products remaining from the manufacturing process, individual higher-concentration stock solutions of angiotensin II were prepared in 100% TFE. The solvent was allowed to evaporate overnight, and the desired quantity of dried product was then re-dissolved in the 50:50 (%volume) TFE:water solution for analysis.<sup>33</sup> For experiments involving thermal incubation of the analyte, samples were stored in polypropylene tubes and placed into a water bath held at a constant temperature of 37 °C (310K).

### Data Analysis

To obtain a more detailed understanding of aggregate formation, IMS–MS measurements were repeated every thirty minutes for a total of 660 minutes. After the first eleven hours, additional experiments were performed over shorter ranges at longer incubation times of 1640 to 1700, 2425 to 2485, and 7490 to 7550 minutes in similar 30 minute intervals. One final experiment was also performed after an incubation time of 9075 minutes, representing a total experimental observation time of approximately six days and seven hours ( $\sim$ 6.3 days). Extracted drift profiles were then obtained by integrating the total ion signal at all drift times for a narrow range of mass-to-charge (m/z) values. The total integrated signal for each ion in the extracted drift profile was then calculated and normalized after accounting for instrumental noise. In order to observe

the long time steps on the same plot as the many shorter time measurements within the first 11 hours, incubation time is represented on a logarithm scale.

#### **Results and Discussion**

Preliminary Aggregation Observations.

A representative two-dimensional (2D) nested dataset is shown in Figure 3.2. Individual ionic species are separated in the drift dimension according to molecular conformation, where elongated conformations have longer drift times than compact conformations as a result of an increased number of collisions with the He buffer gas, and ionic charge state, where a higher charge state has a greater interaction with the applied electrical field. Thus, drift time is proportional to the cross-section of the ion, and inversely proportional to the charge on the ion.

Electrospray ionization of angiotensin II in a 50:50 (% volume) solution of TFE:water produces relatively few major features (Figure 3.2). By far the most abundant feature observed is the  $[M+2H]^{2+}$  ion at ~17 ms ( $m/z \sim 524$ ), followed by the  $[M+3H]^{3+}$  ion at ~13 ms ( $m/z \sim 350$ ). Several other low-intensity unidentified fragment ions are also observed across a wide range of m/z below ~ 800. These two main features are rather unremarkable here, as they are relatively easily produced in a wide variety of electrospray solvents and conditions. Furthermore, neither of them exhibit evidence for the existence of multiple conformations in the gas phase such as those observed in other systems such as bradykinin. <sup>34, 35</sup> Notably, multiple lower-intensity features are observed across a wide range of drift times at  $m/z \sim 1046$ . Initially, prior to IMS dispersion, such features were incorrectly identified as the  $[M+H]^+$  ion; examination of the isotopic distribution shows them to be aggregation products of the form  $[nM+nH]^{n+}$ , where  $(3 \le n \le 1)$ .

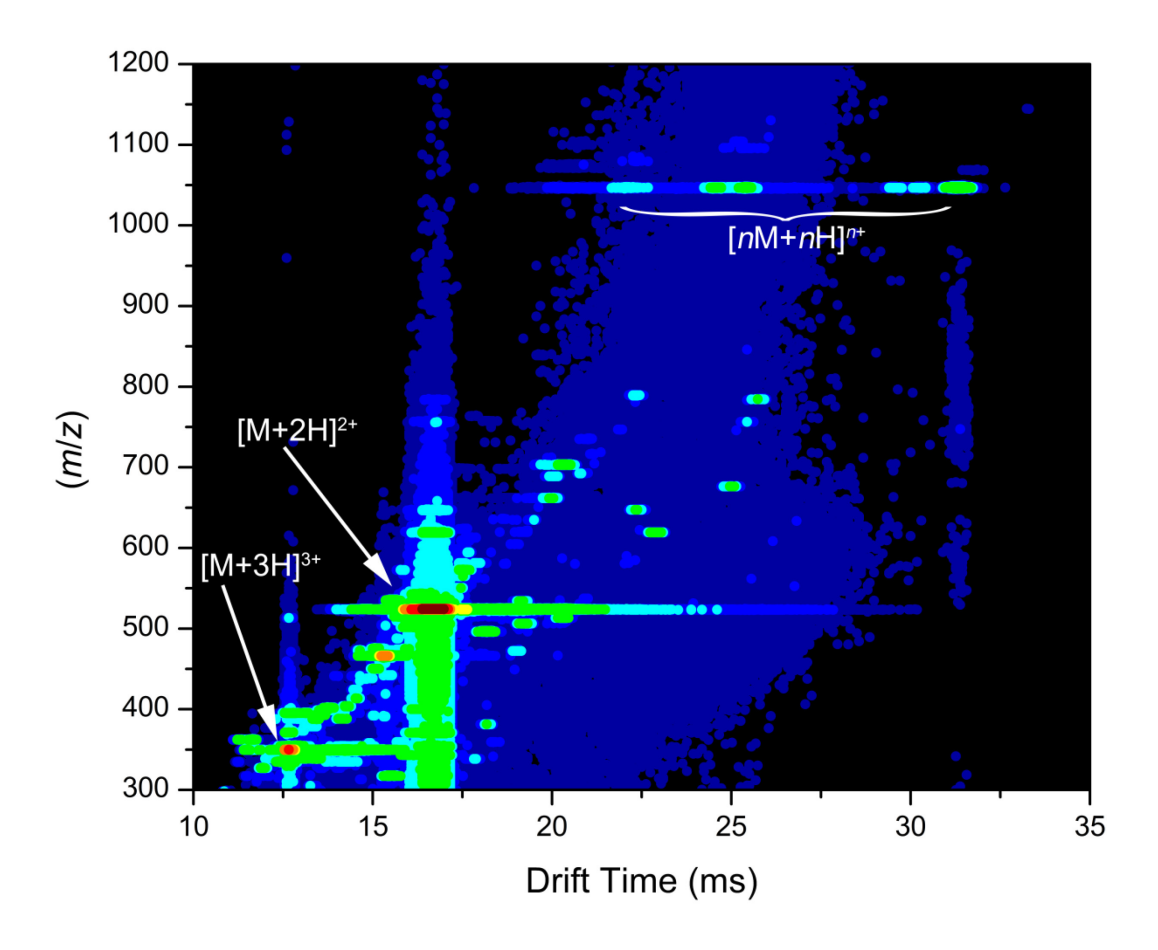
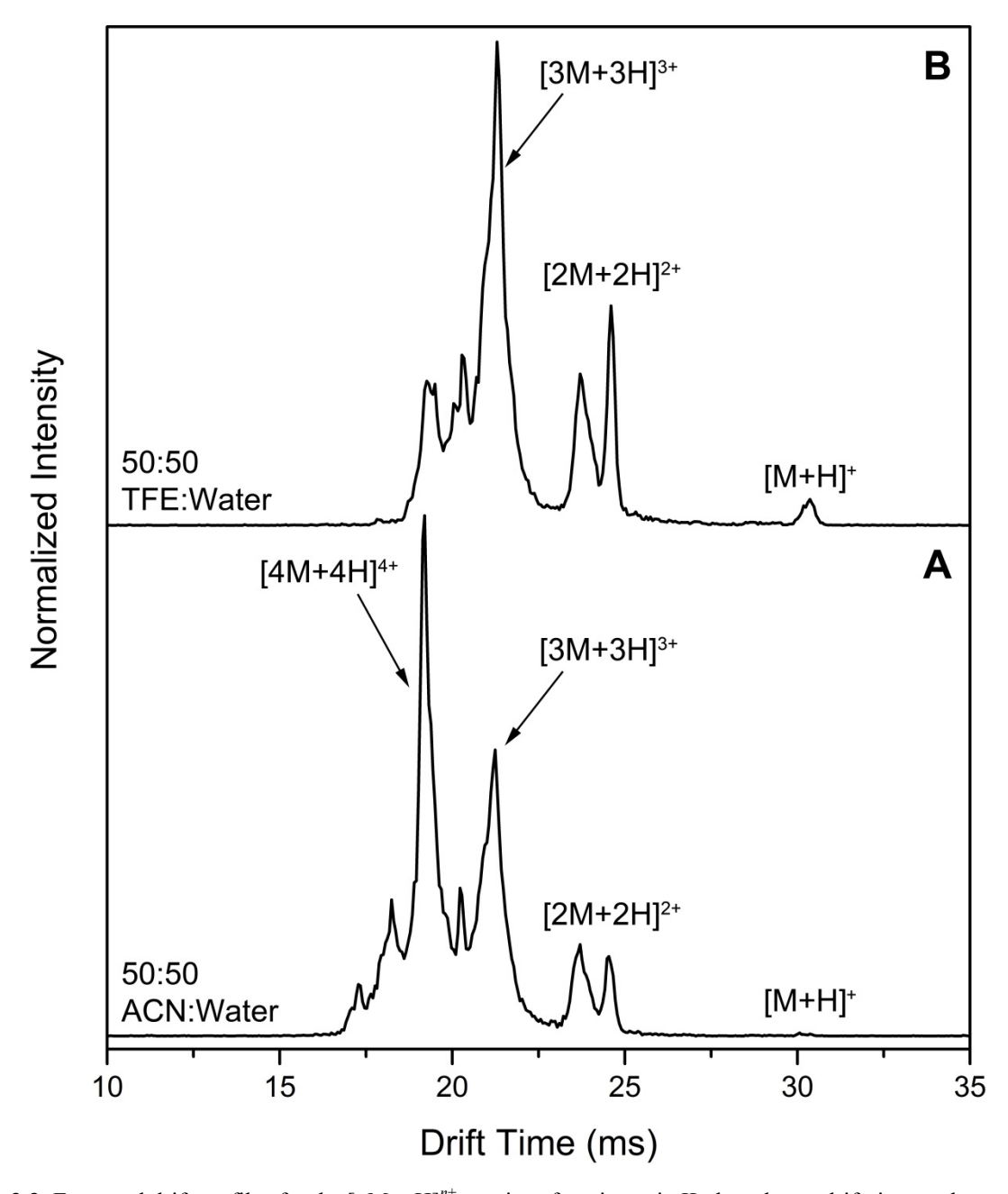


Figure 3.2: Characteristic two-dimensional (2D) representation of mass-to-charge (m/z) ratio measurements nested within drift time measurements for the 60 minute incubation experiment. The three charge states of interest are labeled accordingly and relative signal intensity is represented by color, where cooler colors such as navy blue represent low ion counts and reds indicate high ion counts. The drift pressure was held constant at  $\sim 3.10$  Torr He.

Figure 3.3A shows a drift profile for a limited range ( $m/z \sim 1046-1048$ ) of ions with m/z ratios surrounding that of the [M+H]<sup>+</sup> ion that have been extracted from experiments involving angiotensin II in a 50:50 (by volume) solution of ACN:water. Very little of the monomer species is observed, however relatively high intensities are observed for higher order multimers including the trimer and the tetramer species. Conversely, the use of TFE in place of ACN results in a relative increase from < 1% peak intensity in ACN to ~5% relative intensity in TFE for the monomer species, and a significantly reduced intensity from the dominant feature in ACN, to ~30% relative intensity in TFE for the peak representing the tetramer (Figure 3.3B).

Both solvents allow for the formation of two distinct dimer conformers (Figure 3.3); however the relative intensities of each feature differ slightly, where these relative peak heights are approximately equal in the ACN solution ( $\sim$ 17% and 15%) and noticeably disparate when the electrospray solution contains TFE ( $\sim$ 45% and 31%). Here, although the lack of baseline resolution for the set of dimer populations in both solvents limits the accuracy of peak integration calculations, it is noted that the higher mobility (lower drift time) feature is significantly broader than the lower mobility (higher drift time) feature. In solutions of TFE (Figure 3.3B), the more elongated (lower mobility) conformer exists as a narrow distribution centered at a drift time of 24.6 ms with a peak width of  $\sim$ 0.54 ms. An additional less intense, but wider, feature is observed for a higher mobility conformer centered at 23.8 ms with a full width at half-max (FWHM) of  $\sim$ 0.78 ms. In solutions containing acetonitrile the two peaks have relatively similar heights, although the peak width varies slightly (FWHM  $\sim$ 0.48 and  $\sim$ 0.90 ms, respectively).



**Figure 3.3**: Extracted drift profiles for the  $[nM+nH]^{n+}$  species of angiotensin II plotted on a drift time scale. Experiments were performed with individual  $\sim 0.95$  mM solutions containing equal parts (by volume) ACN and water or TFE and water. Multimer identification is possible by extracting the mass spectral data from each of the distributions and analyzing the isotopic distribution. For both experiments the He buffer gas was maintained at a pressure of  $\sim 3.5$  Torr. As shown here, it is possible to identify individual species up to trimers in solutions of TFE and tetramers in solutions of ACN, although evidence for higher-order aggregates is also observed.

Noticeably more intense features are observed for conformations of the [3M+3H]<sup>3+</sup> and [4M+4H]<sup>4+</sup> species (Figure 3.3). In each solution, none of the features identified as higher order multimers are baseline resolved. The shape of the trimer peak is similar in both solution conditions, including the presence of a leading shoulder, although it is significantly larger and dominant in solutions containing trifluoroethanol. Significant differences are observed for features corresponding to the tetramer, as it is the dominant peak in the extracted drift profile for angiotensin II in the acetonitrile solution, but somewhat poorly resolved in solutions of TFE. Comparatively, the trimer and tetramer features have similar peak widths in solutions containing ACN (~1.14 and ~1.26 ms, respectively). Ultimately, it is noted that it is the dominant presence of these aggregates compared to that of the monomer that has motivated further investigation of this system.

In these initial experiments, mobility measurements were collected immediately after solvation of the lyophilized peptide without incubation. A concern is that a large portion, if not all, of these initial aggregation products could be remnants of the manufacturing/purification process. For these experiments we focus on the use of acetonitrile and 2,2,2-trifluoroethanol as notable electrospray solvents, though many others have been recently investigated. Although the use of acetonitrile as an electrospray solvent is fairly common, and often used to prepare standard solutions for calibration purposes, it is also known that the introduction of acetonitrile can result in a partial unfolding of the native structure and thus contribute to the formation of aggregates. This alone may not sufficiently explain the initial presence of large quantities of these oligomers as it is also known that some aggregation products often remain following the manufacturer's purification processes. Trifluoroethanol, though not commonly used as an electrospray solvent,

is often utilized to stabilize or induce elements of secondary structure, such as helices, in peptides through preferential hydrogen bonding along the backbone. This inducement of intramolecular hydrogen bond formation,<sup>39</sup> may contribute to the observed enhancement in formation of the monomer due to disruption of non-covalent intermolecular bonds (Figure 3.3). Nevertheless, in order to accurately measure the formation of oligomers in solution, it is necessary to ensure complete dissociation of possible pre-existing aggregation products.

# Dissociation of Aggregates.

Obtaining reproducible data is a significant difficulty in accurately studying aggregation phenomena. As an example, previous studies of the amyloid  $\beta$ -protein (A $\beta$ ) have reported significant differences in assembly kinetics between samples obtained from various manufacturers or even separate preparation lots from the same manufacturer. Here, it is theorized that some of this irreproducibility occurs as a result of the presence of pre-existing aggregates in the original peptide stocks, which must be removed or dissociated such that a relatively aggregate-free solution is obtained. For these experiments we have opted for a chemical method involving polyfluorinated alcohols as opposed to other physical methods such as molecular weight filters or size exclusion chromatography (SEC).

Illustrative results of the dissociation procedure are shown in Figure 3.4 for the  $[nM+nH]^{n+}$  ion of angiotensin II in a 50:50 (by volume) solution consisting of TFE and water. When compared to the same ion from untreated angiotensin II (Figure 3.3), it is clear that nearly all of the initial pre-formed aggregates have been dissociated, leaving only an intense narrow feature representing the  $[M+H]^+$  ion. Also shown here are two additional minor features at the base of

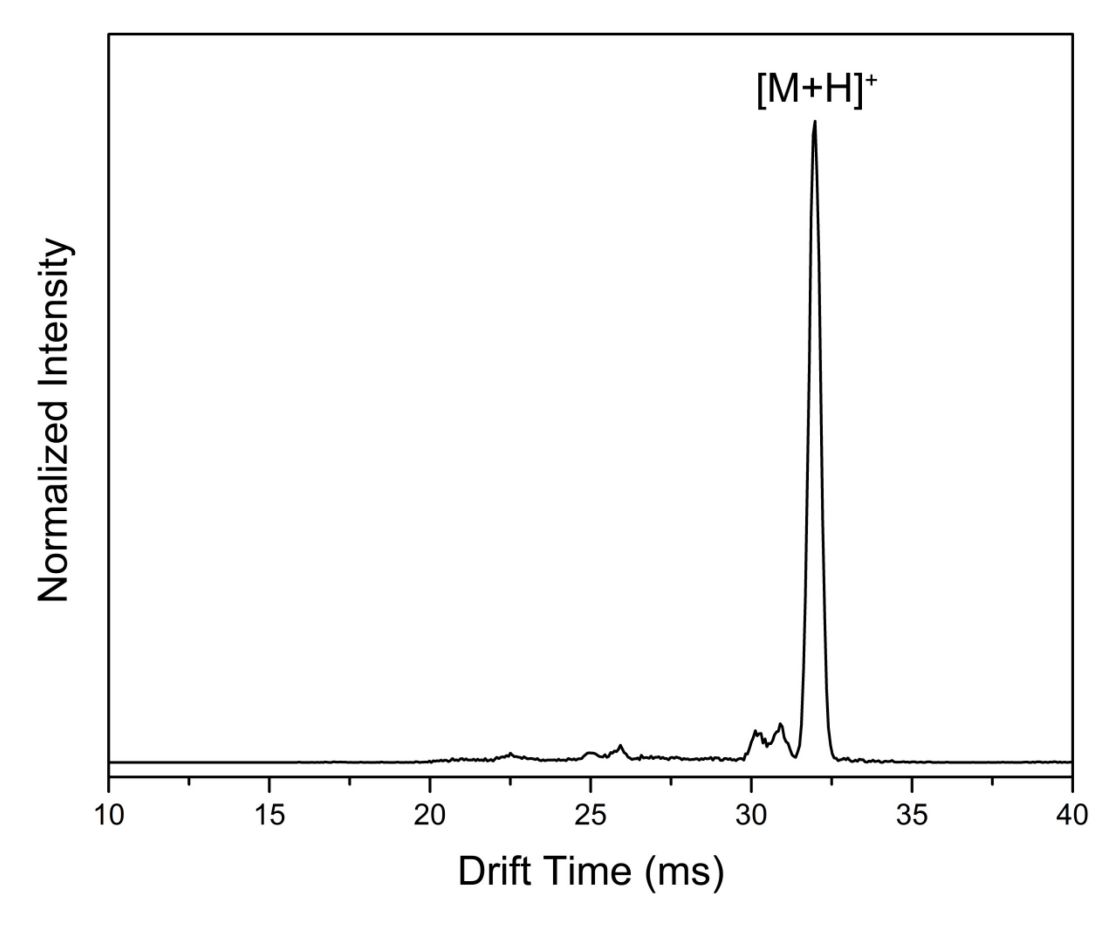


**Figure 3.4**: Extracted drift profile for the  $[nM+nH]^{n+}$  ion of  $\sim 6.8 \times 10^{-4}$  M angiotensin II in 50:50 (% volume) TFE:water after aggregation dissociation treatments. As shown here, the main feature of highest intensity is the singly-protonated monomer (n = 1), however some low intensity residual aggregates are observed as well. The area under the curve is normalized to unity and the He buffer gas was maintained at a pressure of  $\sim 3.15$  Torr.

the  $[M+H]^+$  distribution. These two small distributions with drift times of ~30 and 31 ms represent previously unobserved compact features of the  $[M+H]^+$  ion as confirmed by analysis of their isotopic distributions. It is noted that these features are only observed at relatively high concentrations (~0.8 to 1.0 mg·mL<sup>-1</sup>) in solvents such as TFE and HFIP. With sample incubation, these two low intensity features are lost.

# Time-Dependent Formation of Aggregates.

Once the preexisting aggregates have been dissociated, leaving only a majority of monomers in solution, it is possible to monitor the conversion of these monomers into higher order aggregates. In an attempt to observe an accurate representation of multimer formation as a function of time, ion mobility measurements were utilized to monitor the changes in each of the ion populations as shown in Figure 3.5. Initially, extracted drift profiles were dominated by the  $[M+H]^+$  ion. After incubating the sample at 37 °C (310 K) the population of the monomer quickly decreased relative to other observed features. Furthermore, the observed  $\sim 80\%$  decrease in the intensity of the  $[M+H]^+$  monomer peak ( $\sim 31$  ms) from 60 minutes to 660 minutes is accompanied by comparative increases of  $\sim 130\%$  in the intensity of the compact  $[2M+2H]^{2+}$  feature and an increase of  $\sim 80\%$  in the peak height for the  $[3M+3H]^{3+}$  ion over the same incubation period, suggesting the formation of these aggregate species in solution prior to ionization. Only a small increase of < 30% is observed for the elongated  $[2M+2H]^{2+}$  ion.

As shown in Figure 3.6 the population of the [M+H]<sup>+</sup> monomer decreases over the first 11 hours of the experiment, and then stabilizes at a level slightly below 10% of the total population. While the population of the monomer stabilizes, the populations of the compact [2M+2H]<sup>2+</sup> and

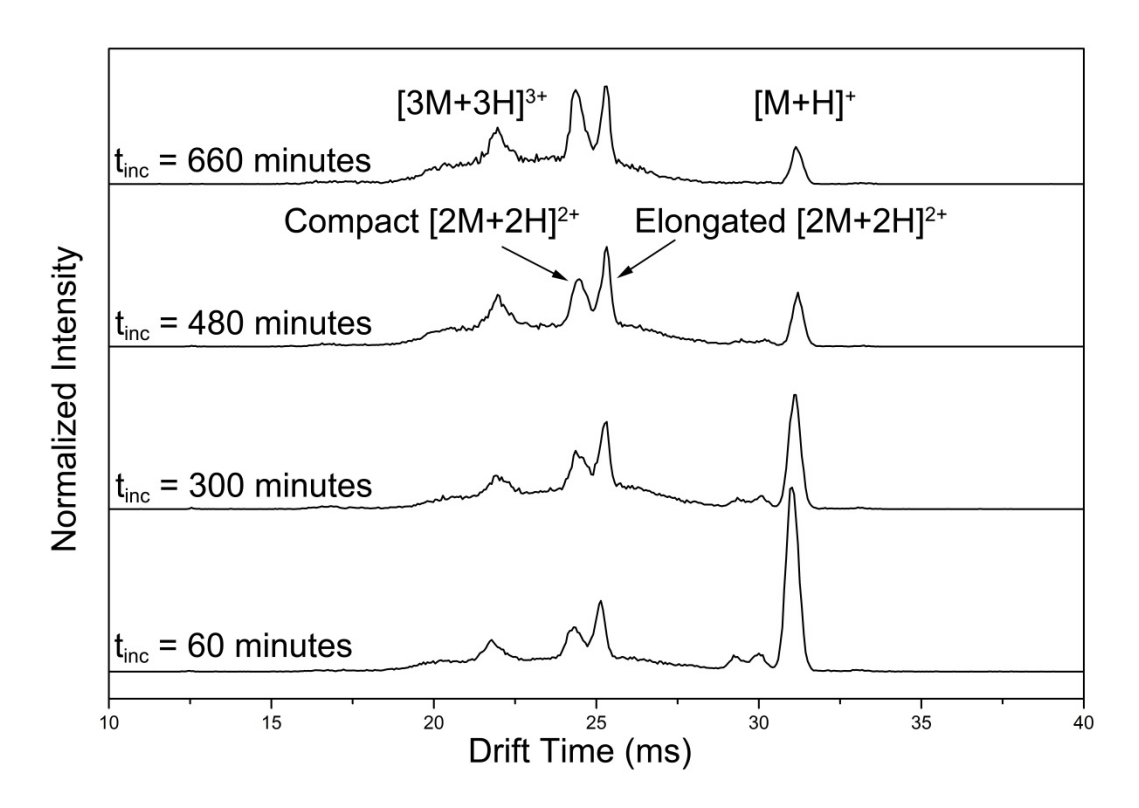


**Figure 3.5**: Extracted drift profiles for the  $[nM+nH]^{n+}$  ion of  $\sim 8.5 \times 10^{-4}$  M angiotensin II in 50:50 TFE:water after dissociation of pre-formed aggregates as a function of incubation time ( $t_{inc}$ ). As shown here, the main feature of the highest intensity is the protonated monomer (n = 1), however some residual aggregates are observed as well. The area under each curve is normalized to unity where each curve is represented on an equivalent scale. The He buffer gas was maintained at a pressure of  $\sim 3.10$  Torr.

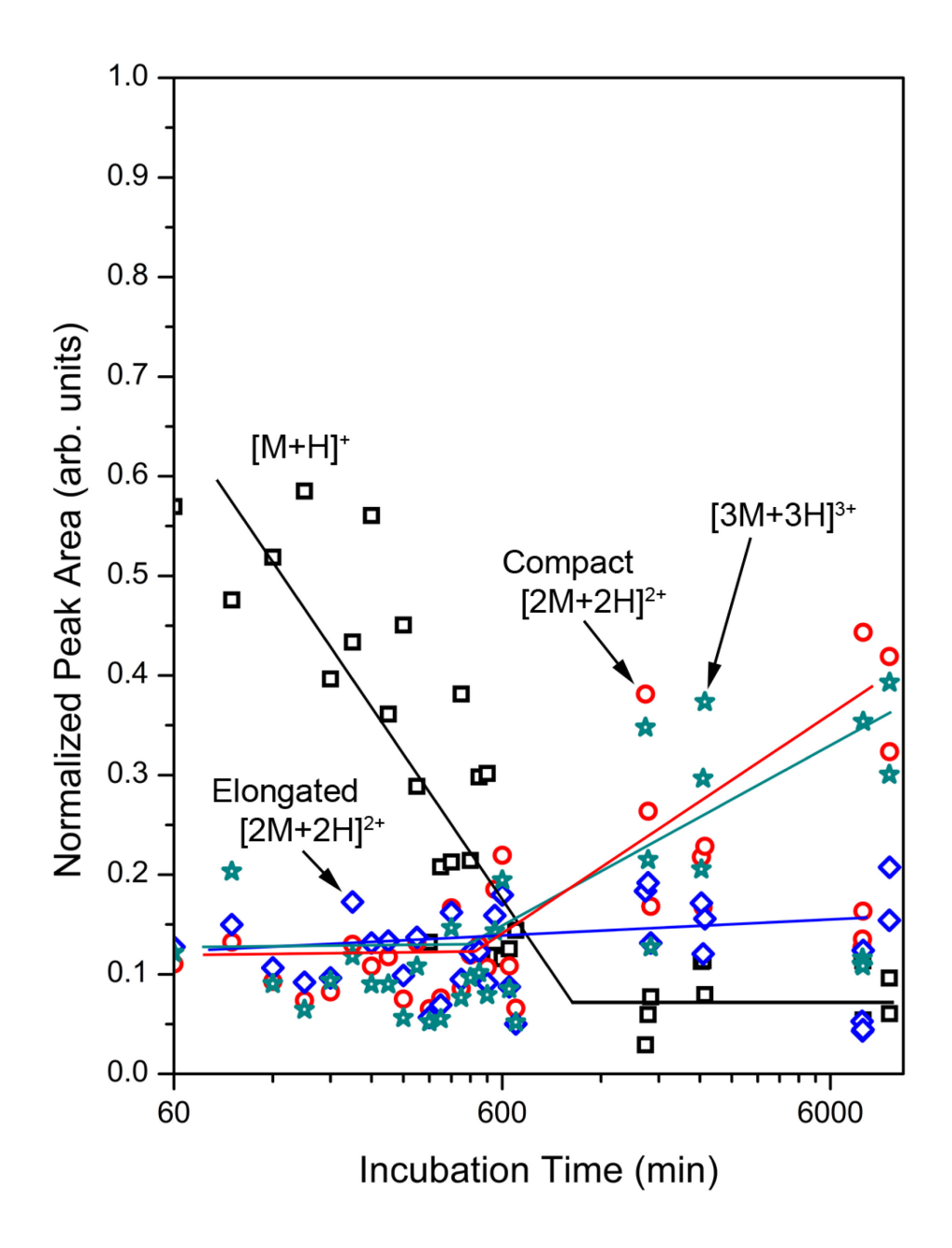


**Figure 3.6**: Calculated and normalized peak area represented as a function of incubation time for each of the four species of angiotensin II of interest. Significantly more measurements are included for the first 660 minutes than for the ~8400 minutes that follow. In order to observe the long time steps on the same plot as the many shorter time measurements within the first 11 hours, incubation time is represented on a logarithm scale. The overlaid lines are not intended to be accurate curve fits, but are only included in order to draw attention to the approximate trends within the data points for illustrative purposes.

 $[3M+3H]^{3+}$  ions start to increase significantly, ultimately combining to account for approximately 80% of the total  $[nM+nH]^{n+}$  signal. Of note, the population of the elongated form of the  $[2M+2H]^{2+}$  dimer remains relatively constant at ~12 to 15% throughout the entire experiment. It is possible that this specific conformation is relatively stable in solution over the time period of the experiment and may not participate in the aggregate transformation (i.e. the shift to higher order aggregates). The high amount of noise in the measurements makes it difficult to precisely fit the data (Figure 3.6); however the overall trends for the different species is still distinguishable.

# Considerations for Further Investigation

A significant difficulty in measuring these aggregates is related to the formation of the multiple monomer ions of the form  $[M+nH]^{n+}$  ( $1 \le n \le 3$ ) during the electrospray process. Instead of observing a single monomer species,  $[M+H]^+$ , three separate ions  $[M+H]^+$ ,  $[M+2H]^{2+}$ , and  $[M+3H]^{3+}$  are formed due to the number of basic sites within the molecule as well as its ability to stabilize increased charge. For angiotensin II, two of the eight residues are commonly considered to be charge-carrying sites within the molecule in addition to the N-terminus,  $^{30}$  for a monomer ion with a theoretical maximum charge of 3+ at pH  $\sim$ 7. The formation of these higher charge state species during the ionization process introduces a complication into the analytical procedure, in that it requires monitoring three separate ion populations in order to accurately account for the entire population of the monomer species extracted from solution. Therefore, to further increase the overall accuracy of these oligomerization measurements, it may be necessary to utilize a solvent system that can be used to favor the formation of lower charge state ions during the electrospray process.

Recent work by Williams and co-workers has shown that it is possible to effectively reduce the charge states for small peptides by introducing a solvent mixture containing organic solvents with relatively high gas-phase basicities. 41 Their initial work utilized several solvents which have already been shown not to favor the formation of the [M+H]<sup>+</sup> ion of angiotensin II, however as is the case with acetonitrile — an increase in higher-order aggregation products is observed. Although this does make it more difficult to observe any transitions from monomers into dimers, trimers, and tetramers that may occur in solution, an increase in overall ion signal for the larger oligomers would allow for higher order tandem IMS-IMS-MS experiments in order to further investigate the gas-phase structures of these multimers. Another experiment proposed by Williams is to simply dope a small quantity of a higher volatility solvent such as diethylamine into the electrospray solution to act as a proton acceptor, reducing the population of available charge carriers. 41 However, as observed in previous experiments with dimethyl sulfoxide, there are some caveats to consider when selecting novel low volatility and high gas phase basicity solvents, especially when they may further complicate the observed spectrum by inducing the formation of new structures, or become preferentially ionized themselves, resulting in an overall decrease in signal for the ions of interest.

#### **Conclusions**

IMS–MS has been used to measure the time-dependent formation of angiotensin II  $[nM+nH]^{n+}$  multimer ions formed by direct ESI. This method has allowed for real-time monitoring of aggregate formation without the loss of structural information typically observed in solution-based methods such as gel electrophoresis. Two distinct conformations of the  $[2M+2H]^{2+}$  ion are formed, one of which appears to be actively involved in the aggregation process. Furthermore, an

~83% decrease in the population of the [M+H]<sup>+</sup> monomer species after more than six days of incubation is observed along with an accompanying four-fold increase in the populations of [2M+2H]<sup>2+</sup> and [3M+3H]<sup>3+</sup> ion species. The observation of two distinct dimer conformations, which are not resolved with other methods, demonstrates the importance of IMS as a structural characterization technique.

# Acknowledgements

This work is supported in part by the Indiana University METAcyte initiative, which receives funding from grants provided by the Lilly Endowment.

#### References

- 1. Kirkitadze, M. D.; Bitan, G.; Teplow, D. B., *J. Neurosci. Res.* **2002**, *69*, 567–577.
- 2. Lashuel, H. A.; Hartley, D.; Petre, B. M.; Walz, T.; Lansbury, P. T., *Nature* **2002**, *418*, 291–291.
- 3. Kłoniecki, M.; Jabłonowska, A.; Poznański, J.; Langridge, J.; Hughes, C.; Campuzano, I.; Giles, K.; Dadlez, M., *J. Mol. Biol.* **2011**, *407*, 110–124.
- 4. Thirumalai, D.; Klimov, D.; Dima, R., Curr. Opin. Struct. Biol. 2003, 13, 146–159.
- 5. Fenn, J. B.; Mann, M.; Meng, C. K.; Wong, S. F.; Whitehouse, C. M., *Science* **1989**, *246*, 64–71.
- 6. Lee, S.-W.; Freivogel, P.; Schindler, T.; Beauchamp, J. L., *J. Am. Chem. Soc.* **1998**, *120*, 11758–11765.
- 7. Counterman, A. E.; Valentine, S. J.; Srebalus, C. A.; Henderson, S. C.; Hoaglund, C. S.; Clemmer, D. E., *J. Am. Soc. Mass Spectrom.* **1998**, *9*, 743–759.
- 8. Attwood, D.; Florence, A. T.; Greig, R.; Smail, G. A., *J. Pharm. Pharmacol.* **1974**, *26*, 848–853.
- 9. Deslauriers, R.; Paiva, A. C. M.; Schaumburg, K.; Smith, I. C. P., *Biochemistry* **1975**, *14*, 878–886.
- 10. Lenkinski, R. E.; Stephens, R. L.; Krishna, N. R., *Biochemistry* **1981**, *20*, 3122–3126.
- 11. Gerig, J. T., J. Phys. Chem. B **2008**, 112, 7967–7976.
- 12. Greff, D.; Fermandjian, S.; Fromageot, P.; Khosla, M. C.; Smeby, R. R.; Rumpus, F. M., *Eur. J. Biochem.* **1976**, *61*, 297-305.
- 13. Rabilloud, T., *Proteomics* **2002**, *2*, 3–10.
- 14. Bhuyan, A. K., *Biopolymers* **2010**, *93*, 186–199.

- 15. Mack, E., J. Am. Chem. Soc. 1925, 47, 2468–2482.
- 16. Revercomb, H. E.; Mason, E. A., *Anal. Chem.* **1975**, *47*, 970–983.
- 17. Mason, E.; McDaniel, E., *Transport Properties of Ions in Gases*. Wiley: New York, 1988.
- 18. Shvartsburg, A. A.; Jarrold, M. F., Chem. Phys. Lett. 1996, 261, 8691.
- 19. Mesleh, M. F.; Hunter, J. M.; Shvartsburg, A. A.; Schatz, G. C.; Jarrold, M. F., *J. Phys. Chem.* **1996**, *100*, 16082–16086.
- 20. Wyttenbach, T.; Helden, G. v.; Batka, J. J. J.; Carlat, D.; Bowers, M. T., *J. Am. Soc. Mass Spectrom.* **1997**, *8*, 275–282.
- 21. Koeniger, S. L.; Merenbloom, S. I.; Clemmer, D. E., *J. Phys. Chem. B* **2006**, *110*, 7017–7021.
- 22. Wittmer, D.; Chen, Y. H.; Luckenbill, B. K.; Hill, H. H., *Anal. Chem.* **1994**, *66*, 2348–2355.
- Gillig, K. J.; Ruotolo, B.; Stone, E. G.; Russell, D. H.; Fuhrer, K.; Gonin, M.; Schultz, A. J., *Anal. Chem.* 2000, 72, 3965–3971.
- 24. Hoaglund, C. S.; Valentine, S. J.; Sporleder, C. R.; Reilly, J. P.; Clemmer, D. E., *Anal. Chem.* **1998**, *70*, 2236–2242.
- 25. Hoaglund-Hyzer, C. S.; Li, J.; Clemmer, D. E., Anal. Chem. 2000, 72, 2737–2740.
- Valentine, S. J.; Kulchania, M.; Barnes, C. A. S.; Clemmer, D. E., *Int. J. Mass. Spectrom.* 2001, 212, 97–109.
- 27. Tang, K.; Shvartsburg, A. A.; Lee, H.-N.; Prior, D. C.; Buschbach, M. A.; Li, F.; Tolmachev, A. V.; Anderson, G. A.; Smith, R. D., *Anal. Chem.* **2005**, *77*, 3330–3339.
- 28. Koeniger, S. L.; Merenbloom, S. I.; Valentine, S. J.; Jarrold, M. F.; Udseth, H. R.; Smith, R. D.; Clemmer, D. E., *Anal. Chem.* **2006**, *78*, 4161–4174.

- 29. Merenbloom, S. I.; Koeniger, S. L.; Valentine, S. J.; Plasencia, M. D.; Clemmer, D. E., *Anal. Chem.* **2006**, *78*, 2802–2809.
- 30. Hoaglund-Hyzer, C. S.; Counterman, A. E.; Clemmer, D. E., *Chem. Rev.* **1999**, *99*, 3037–3079.
- 31. Shaffer, S. A.; Tang, K.; Anderson, G. A.; Prior, D. C.; Udseth, H. R.; Smith, R. D., Rapid Commun. Mass Spectrom. 1997, 11, 1813–1817.
- 32. Shaffer, S. A.; Prior, D. C.; Anderson, G. A.; Udseth, H. R.; Smith, R. D., *Anal. Chem.* **1998**, *70*, 4111–4119.
- 33. Rahimi, F.; Maiti, P.; Bitan, G., J. Vis. Exp. **2009**, 23, e1071.
- 34. Pierson, N. A.; Valentine, S. J.; Clemmer, D. E., J. Phys. Chem. B **2010**, 114, 7777–7783.
- 35. Pierson, N. A.; Chen, L.; Valentine, S. J.; Russell, D. H.; Clemmer, D. E., *J. Am. Chem. Soc.* **2011**, *133*, 13810–13813.
- 36. Shi, H.; Pierson, N.; Valentine, S.; Clemmer, D. E., *J. Phys. Chem. B* **2012**, *116*, 3344–3352.
- 37. Amani, S.; Naeem, A., Int. J. Biol. Macromol. **2011**, 49, 71–78.
- 38. Cromwell, M. E. M.; Hilario, E.; Jacobson, F., *AAPS J.* **2006**, *8*, E572–579.
- 39. Buck, M., Q. Rev. Biophys. 1998, 31, 297–355.
- 40. Bitran, G.; Teplow, D. B., Methods Mol. Biol 2005, 299, 3-9.
- 41. Iavarone, A. T.; Jurchen, J. C.; Williams, E. R., *J. Am. Soc. Mass Spectrom.* **2000**, *11*, 976–985.

# Appendix A

In order to fully understand the influence of electrospray solvent on both solution- and gas-phase biomolecular conformations, it is instructive to consider some of the important physical properties of the organic solvents utilized in the previous experiments. Table A.1 lists the five organic solvents that were investigated as part of the experiments discussed in Chapters 2 and 3, as well of that of high-purity water, which is a component of all of the solvent systems that have been explored.

Solvents such as acetonitrile and methanol were included in these experiments as a control. Both of these solvents are commonly used in liquid chromatography/mass spectrometry (LC/MS) experiments, where their usefulness as electrospray ionization (ESI) solvents can be utilized as well. Dioxane (*p*-dioxane or 1,4-dioxane) is a less common ESI solvent, but it has been shown to induce some conformational changes in peptides as illustrated in previous experiments with bradykinin. Therefore, it has been included as part of these studies in an attempt to expand upon the findings of the first investigation, although as explained previously, it does not appear to have the same kind of effect on the structure of angiotensin I that it does on that of bradykinin. It is also instructive to note that the small dipole moment (0.05 D) observed for 1,4-dioxane is a result of structural interconversion between the chair and boat conformations of the six-membered ring.

The use of dimethyl sulfoxide (DMSO) as an electrospray solvent is not a novel concept, as it is often used in small amounts in order to increase solubility, or in more recent studies, to induce structural changes allowing for the formation of higher charge states.<sup>3</sup> Of the solvents examined

**Table A.1**: Tabulated physical properties of the six analytical solvents investigated during the course of the experiments described in Chapter 2 and Chapter 3.

Solvent	Structure	Dielectric Constant (ε <sub>r</sub> , 20°C)*	Dipole Moment <sup>†</sup> (D) <sup>‡</sup>	Proton Affinity <sup>§</sup> (kJ/mol)	Gas Phase Basicity <sup>§</sup> (kJ/mol)
Water	H .O.	80.29	1.85	691.0	660.0
Methanol	H <sub>3</sub> C H	33.64	1.70	754.3	725.5
1,4-Dioxane		2.22	0.05**	794.4	770.0
Acetonitrile	: N === C CH <sub>3</sub>	36.78	3.93	779.2	748.0
Trifluoroethanol	CF <sub>3</sub> :Ö——CH <sub>2</sub>	27.79	$2.46^{\dagger\dagger}$	700.2	669.9
Dimethyl sulfoxide	H <sub>3</sub> C CH <sub>3</sub>	47.13	3.96	884.4	853.7

\_

<sup>\*</sup> Wohlfarth, C., Static Dielectric Constants of Pure Liquids and Binary Liquid Mixtures, *Landolt-Bornstein, Numerical Data and Functional Relationships in Science and Technology, New Series*, Editor in Chief, O. Madelung, Group IV, Macroscopic and Technical Properties of Matter, Volume 17, Springer-Verlag, Berlin, 2008.

<sup>&</sup>lt;sup>†</sup> CRC Handbook of Chemistry and Physics. 91st ed. CRC Press: Boca Raton, FL, **2010-2011**; p 9-51–59.

 $<sup>^{\</sup>ddagger}$  1 debye unit (D) = 3.33564×10<sup>-30</sup> C·m

<sup>§</sup> E. Hunter and S. Lias, J. Phys. Chem. Ref. Data, 1998, 27(3), 413-656.

<sup>\*\*\*</sup> Jensen, L.; van Duijnen, P. T., *J. Chem. Phys.* **2005**, *123* (7), 074307–7.

<sup>&</sup>lt;sup>††</sup> Mainar, A. M.; Pardo, J.; Royo, F. M.; López, M. C.; Urieta, J. S., *J. Solution Chem.* **1996**, *25* (6), 589–595.

here, DMSO is the only one with a lower volatility (higher vaporization temperature) than water. This lower volatility may result in longer interaction times with the peptide, as DMSO evaporates last during the electrospray process. However, it is more likely that the both solvents (DMSO and water) are lost simultaneously as the peptide molecule is ejected from the droplet. Furthermore, the preferential ionization of DMSO at higher concentrations can be explained by its relatively large proton affinity and gas phase basicity. Although these values are still significantly lower than those associated with the common basic residues (Lys, Arg, His),<sup>4</sup> the large number of available DMSO molecules relative to peptide molecules may explain why we do not observe any peptide ions at high concentrations of DMSO.

Trifluoroethanol (TFE) is a relatively uncommon ESI solvent; however it is fairly common in biology as a co-solvent for the study of protein folding in NMR.<sup>5-7</sup> TFE, and other fluorinated alcohols such as hexafluoroisopropanol (HFIP), have the interesting ability to induce conformational changes, including the formation of  $\alpha$ -helices, in the peptide.<sup>5, 8</sup> Some preliminary modeling studies involving angiotensin II in solutions of TFE suggest that we may have observed similar results in our gas phase experiments, though it is necessary to continue this work further before coming to any solid conclusions.

Although it is difficult to definitively associate any of these individual physical properties with associated experimental observations, it is instructive to consider them as part of the experimental variables. As such, this brief discussion exists outside of the scope of the main experimental results and discussion in an attempt to guide further investigations. For example, it may be informative to perform similar experiments with a solvent with a higher gas phase

basicity and proton affinity such as diethylamine, or a solvent with a lower dipole moment such as carbon disulfide.

# References

- 1. Keppel, T. R.; Jacques, M. E.; Weis, D. D., Rapid Commun. Mass Spectrom. 2010, 24, 6-10.
- 2. Pierson, N. A.; Chen, L.; Valentine, S. J.; Russell, D. H.; Clemmer, D. E., *J. Am. Chem. Soc.* **2011**, *133*, 13810–13813.
- 3. Sterling, H.; Prell, J.; Cassou, C.; Williams, E., *J. Am. Soc. Mass Spectrom.* **2011**, *22*, 1178–1186.
- 4. Harrison, A. G., Mass Spectrom. Rev. 1997, 16, 201–217.
- 5. Roccatano, D.; Colombo, G.; Fioroni, M.; Mark, A. E., *Proc. Natl. Acad. Sci. U. S. A.* **2002**, *99*, 12179–12184.
- 6. Hong, D.-P.; Hoshino, M.; Kuboi, R.; Goto, Y., *J. Am. Chem. Soc.* **1999**, *121*, 8427–8433.
- 7. Jasanoff, A.; Fersht, A. R., *Biochemistry* **1994**, *33*, 2129–2135.
- 8. Roccatano, D.; Fioroni, M.; Zacharias, M.; Colombo, G., *Protein Sci.* **2005**, *14*, 2582–2589.

# Appendix B

#### Introduction

Increases in computing power and efficiency have led to remarkable growth in the capabilities of molecular modeling and simulation programs. This advancement in computational power allows rapid development of molecular models corresponding to experimental observations, and the ability to visualize phenomena that may not be detectable through other methods. Although ion mobility spectrometry (IMS) allows us to measure collisional cross-sections (CCS) for gas-phase molecular conformations (Equation 2.1), it does not provide complete structural information. Therefore, it is necessary to utilize additional outside techniques in order to create viable theoretical structures and conformations with cross-sections that match those determined experimentally. To that end, we use currently available high-speed parallel computing resources to perform molecular dynamics (MD) calculations on angiotensin I in a solvent environment containing a mixture of dimethyl sulfoxide (DMSO) and water.

#### **Experimental**

#### General

Molecular dynamics simulations were performed using NAMD,<sup>2</sup> a parallel MD code based on Charm++ parallel objects. A PDB structure file for the solvent system (50:50 %volume DMSO:water) was prepared using 2396 individual TIP3 water and 611 DMSO structure files inside a 72,000 Å<sup>3</sup> (40x40x45Å) rectangular box using Packmol,<sup>3</sup> such that the density of the solution within the box was approximately equal to that calculated for the actual solution mixture. A structure file for angiotensin I was obtained from the Protein Data Bank (1N9U)<sup>4</sup> and inserted into the center of the solvent box using VMD.<sup>5</sup> Once the peptide structure was placed within the solvent box, complete coordinate (PDB) and solvation (PSF) files were generated with

VMD. A separate solvent system was also created without DMSO by solvating the angiotensin I (1N9U) structure coordinate file with only water molecules.

#### NAMD Parameters

NAMD calculations were performed at 300 K under a constant pressure of 101.325 kPa for 10 to 20 ns. Parameters for the water molecules, and the amino acid residues in angiotensin I were obtained from the combined CHARMM all-hydrogen parameter files for CHARMM22 Proteins and CHARMM27 Nucleic Acids.<sup>6</sup> Similar parameters for DMSO were obtained from CGenFF (v2b7).<sup>7</sup>

#### Collisional Cross-Section Calculation

Upon completion of the MD simulations, individual coordinate files for the peptide were extracted from the solvated file using VMD. For the DMSO:water system 4000 separate peptide structure files were obtained. The calculation for the peptide in pure water was allowed to run for half of the time allotted the mixed solvent system, so only 2000 separate files were collected. Collisional cross-sections for each of the conformations were calculated using a modified version of Mobcal<sup>8, 9</sup> that had been updated to FORTRAN95 and compiled for Microsoft® Windows. Mobcal is capable of calculating cross-sections in three different ways: Projection Approximation (PA), Exact Hard Sphere Scattering (EHSS) and the Trajectory Method (TM). For all cross-section calculations here, the trajectory method has been used.

# **Preliminary Results and Discussion**

A plot of calculated collisional cross-section (CCS) verses simulation time can be seen in Figure B.1, where the red line represents all 4000 calculated conformations, and the black line represents a moving average of the ten nearest neighbors ( $t \pm 0.025$  ns). At low time points, the

calculation is working to minimize the energy of the system, so the starting cross-section is relatively large; however, as the energy of the system is minimized, a reduction in cross-section is observed. Finally, at long simulation times, a stabilization of the calculated cross-section is observed between that of the experimentally determined cross-sections for the B and C conformer discussed previously in Chapter 2. It is also observed that under these conditions, no conformations possibly representing that of conformer A are formed. This may be due to the fact that conformer A is a stable gas-phase structure and not directly formed in solution. However, as shown in the inset in Figure B.1, it is possible to form something related to conformer A without the presence of DMSO.

For all of the calculated cross-sections, the trajectory method has been used.<sup>8</sup> It is typically the most accurate, but also the most computationally demanding, often resulting in significantly longer computational time requirements relative to the other methods. It is instructive to explain here that the trajectory method treats the ion itself as a collection of atoms, each of which is represented by a Leonard-Jones (12-6-4) potential.<sup>8, 9</sup> These individual potentials are then summed in order to obtain the effective potential of the ion, which is then used to determine the scattering angle ( $\angle\Theta$  = incoming trajectory – outgoing trajectory) of the incoming buffer gas atoms. The orientationally-averaged collisional cross-section is then determined by integrating over all possible collision geometries.

#### **Conclusions**

Although these molecular modeling results are at a relatively early stage of development, they are helpful in understanding the connection between the experimentally observed gas-phase

conformations, and those simulated in solution. Further investigation will be necessary in order to fully understand these preliminary results.

# Acknowledgements

NAMD was developed by the Theoretical and Computational Biophysics Group in the Beckman Institute for Advanced Science and Technology at the University of Illinois at Urbana-Champaign.

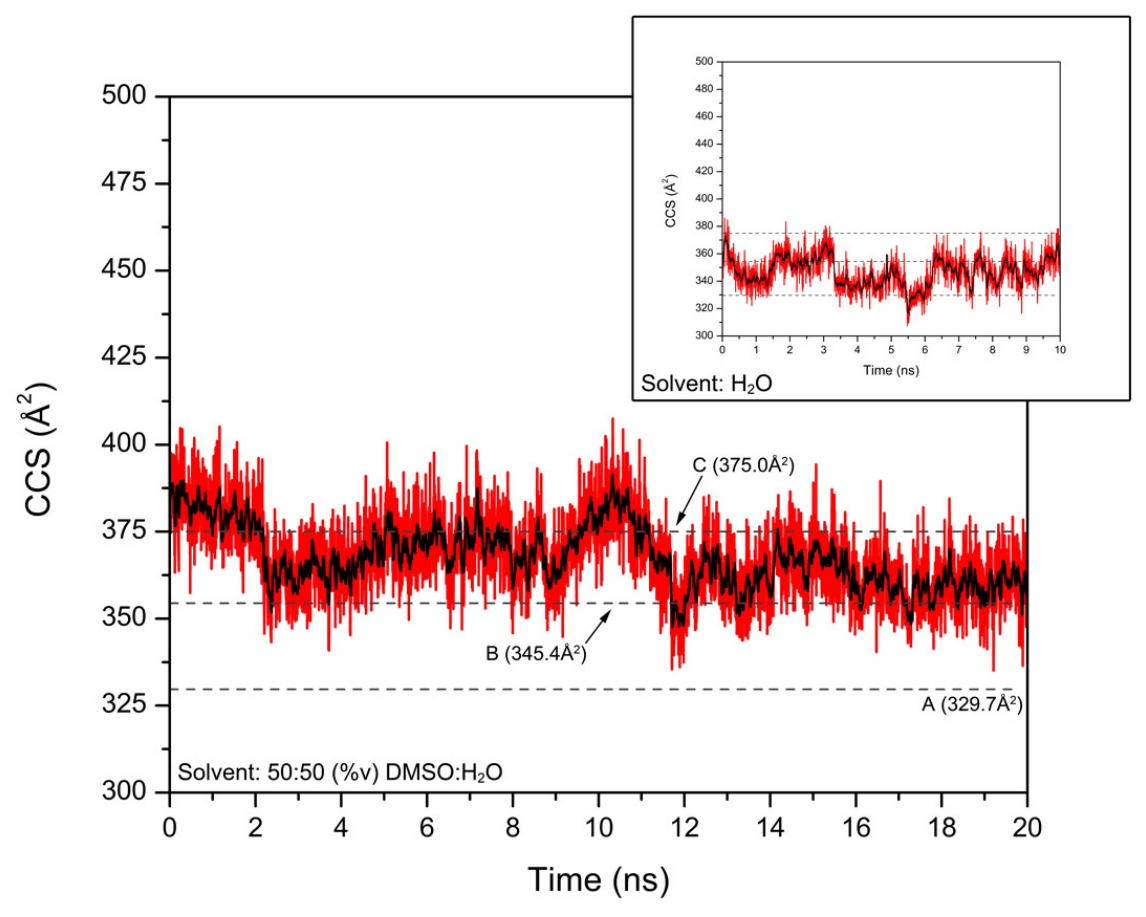


**Figure B.1**: Calculated collisional cross-section (CCS) plotted on a time scale. The red line represents the raw calculations for all 4000 conformations as a function of simulation time. The black line is a moving average (n = 10) illustrating the general trend of the calculations. Dashed lines representing the three experimentally determined collisional cross-sections for each of the conformers (A–C) of angiotensin I in DMSO:water are overlaid. The inset figure shows the same MD calculation performed on a shortened time scale without the presence of DMSO, where an overall decrease in CCS is observed.

#### References

- van Gunsteren, W. F.; Bakowies, D.; Baron, R.; Chandrasekhar, I.; Christen, M.; Daura, X.; Gee, P.; Geerke, D. P.; Glättli, A.; Hünenberger, P. H.; Kastenholz, M. A.; Oostenbrink, C.; Schenk, M.; Trzesniak, D.; van der Vegt, N. F. A.; Yu, H. B., *Angew. Chem. Int. Edit.* 2006, 45, 4064–4092.
- 2. Phillips, J. C.; Braun, R.; Wang, W.; Gumbart, J.; Tajkhorshid, E.; Villa, E.; Chipot, C.; Skeel, R. D.; Kalé, L.; Schulten, K., *J. Comput. Chem.* **2005**, *26*, 1781–1802.
- 3. L. Martínez; R. Andrade; E. G. Birgin; Martínez, J. M., *J. Comput. Chem.* **2009**, *30*, 2157–2164.
- 4. Spyroulias, G. A.; Nikolakopoulou, P.; Tzakos, A.; Gerothanassis, I. P.; Magafa, V.; Manessi Zoupa, E.; Cordopatis, P., *Eur. J. Biochem.* **2003**, *270*, 2163–2173.
- 5. Humphrey, W.; Dalke, A.; Schulten, K., J. Molec. Graphics 1996, 14, 33–38.
- 6. MacKerell, J., A. D.;; Bashford, D.; Bellott, M.; Dunbrack Jr., R. L.; Evanseck, J. D.; Field, M. J.; Fischer, S.; Gao, J.; Guo, H.; Ha, S.; Joseph-McCarthy, D.; Kuchnir, L.; Kuczera, K.; Lau, F. T. K.; Mattos, C.; Michnick, S.; Ngo, T.; Nguyen, D. T.; Prodhom, B.; Reiher, I., W.E.; ; Roux, B.; Schlenkrich, M.; Smith, J. C.; Stote, R.; Straub, J.; Watanabe, M.; Wiorkiewicz-Kuczera, J.; Yin, D.; Karplus, M., *J. Phys. Chem. B* 1998, 102, 3586–3613.
- 7. Vanommeslaeghe, K.; Hatcher, E.; Acharya, C.; Kundu, S.; Zhong, S.; Shim, J.; Darian, E.; Guvench, O.; Lopes, P.; Vorobyov, I.; Mackerell Jr., A. D., *J. Comput. Chem.* **2010**, *31*, 671–690.
- 8. Mesleh, M. F.; Hunter, J. M.; Shvartsburg, A. A.; Schatz, G. C.; Jarrold, M. F., *J. Phys. Chem.* **1996**, *100*, 16082–16086.
- 9. Shvartsburg, A. A.; Jarrold, M. F., Chem. Phys. Lett. **1996**, 261, 8691.

# **CURRICULUM VITA**

# Jeffrey A. Everett

2835 E. Bressingham Way Bloomington, IN 47401 407.929.0225

#### **Education**

Indiana University, Bloomington, IN

Master of Science in Analytical Chemistry, May 2012

Thesis Title: "Solvent-Induced Changes in Molecular Conformation and Aggregation Studied by Ion Mobility Experiments."

University of Central Florida, Orlando, FL

Bachelor of Science in Forensic Science, Minors in Criminal Justice and Political Science, Certificate in Crime Scene Investigation, August 2008

# **Research Experience**

<u>Indiana University Department of Chemistry</u>: May 2009–May 2012.

Analysis of peptide conformation and the role of electrospray solvent composition in the formation of gas-phase conformations and aggregates with Dr. David E. Clemmer. Gained experience with ion mobility spectrometry and time-of-flight mass spectrometry.

Florida State Bureau of Forensic Fire and Explosive Analysis: May 2008–July 2008.

Analysis of collected fire debris evidence samples collected from suspected arson sites with Carl Chasteen and P. Michael Koussiafes. Examination of collected samples from improvised explosive devices and clandestine methamphetamine production facilities with Michael Koussiafes. Experience with GC–MS, HPLC, and XFR.

#### **Presentations and Publications**

Everett, J.A., Valentine, S.V., Clemmer, D.E. "Influence of Solvent Composition on Gas-Phase Structure of Angiotensin I Determined by Ion Mobility Measurements." Presented at Turkey Run Analytical Conference, October 2011.

Glaskin, R.S., Everett, J.A., Valentine, S.J., "Clemmer, D.E. Increased Ion Capacity of a Circular Drift Tube in Frequency Scanning Mode." Presented at American Society for Mass Spectrometry Conferences (Denver, CO), May 2011.

Everett, J.A., Koussiafes, P.M., "The Determination of the Reusability of Containers in the Analysis of Standard Gasoline and Diesel Fuel Residues Using Passive Headspace Extraction." Presented at Pittcon Conference and Expo (Chicago, IL), March 2009.

# **Manuscripts in Preparation or Under Review**

Everett, J.A., Valentine, S.V., Clemmer, D.E. Aggregation of Angiotensin II Monitored in Real Time by Ion Mobility Spectrometry. (In Progress)

Everett, J.A., Valentine, S.V., Clemmer, D.E. Influence of Solution Composition on Gas-Phase Structure of Angiotensin I Determined by Ion Mobility Measurements. (In Progress)

Everett, J.A., Dilger, J., Valentine, S.J., Shelley, J. and Clemmer, D.E. Improvement of Chemical Detection Selectivity with FAPA–IMS–IMS–MS. (In Progress)

# **Professional Affiliations**

American Chemical Society (member since 2012) American Society for Mass Spectrometry (member since 2011) American Academy of Forensic Science (member 2006–2009)